ELSEVIER

Numerical simulations of the Mediterranean sea outflow: impact of the entrainment parameterization in an isopycnic coordinate ocean model

Matheos P. Papadakis [a], Eric P. Chassignet [a,*], Robert W. Hallberg [b]

[a] *RSMAS/MPO, 4600 Rickenbacker Causeway, University of Miami, Miami, FL 33149-1098, USA*
[b] *NOAA/GFDL, Princeton, NJ 08542, USA*

Abstract

Gravity current entrainment is essential in determining the properties of the interior ocean water masses that result from marginal sea overflows. Although the individual entraining billows will be unresolvable in large-scale ocean models for the foreseeable future, some large-scale simulations are now being carried out that do resolve the intermediate scale environment which may control the rate of entrainment. Hallberg [Mon. Wea. Rev. 128 (2000) 1402] has recently developed an implicit diapycnal mixing scheme for isopycnic coordinate ocean models that includes the Richardson number dependent entrainment parameterization of Turner [J. Fluid Mech. 173 (1986) 431], and which may be capable of representing the gravity current evolution in large-scale ocean models. The present work uses realistic regional simulations with the Miami Isopycnic Coordinate Ocean Model (MICOM) to evaluate ability of this scheme to simulate the entrainment that is observed to occur in the bottom boundary currents downstream of the Mediterranean outflow. These simulations are strikingly similar to the observations, indicating that this scheme does produce realistic mixing between the Mediterranean outflow and the North Atlantic Central Water. Sensitivity studies identify the critical Richardson number below which vigorous entrainment occurs as a particularly important parameter. Some of these experiments also show meddies detaching from the Mediterranean undercurrent at locations that appear to be highly influenced by topographic features.
© 2002 Elsevier Science Ltd. All rights reserved.

Keywords: Mediterranean sea outflow; Meddies; Entrainment; Isopycnic coordinate; Ocean modelling

* Corresponding author. Tel.: +1-305-361-4041; fax: +1-305-361-4696.
E-mail address: echassignet@rsmas.miami.edu (E.P. Chassignet).

1. Introduction

The oceanic thermohaline circulation contributes significantly to the poleward heat transport, thus playing an important role in the ocean's contribution to regulating the earth's climate. The properties of the water masses involved in the thermohaline circulation and the rates at which these water masses are formed are of clear climatic significance. Reliable predictions of climate dynamics require models with physically accurate portrayals of the processes governing both the mean rates and the sensitivities governing the formation of these water masses.

Important dense water formation processes take place in several marginal seas, resulting in the inflow of dense water into the large ocean basins. The dense water overflows at the connecting strait, entering the basin as a bottom density current. As these dense bottom currents flow down the continental slope and into the ocean interior, they entrain mass from the less dense overlying water, thus becoming more buoyant (this process will hereafter be referred to as 'entrainment'). There are three major overflows into the North Atlantic basin: the Denmark Strait overflow, the Faroe Bank Channel overflow, and the Mediterranean overflow. The Mediterranean overflow is perhaps the most complex of the major marginal sea overflows into the North Atlantic, due to its separation into different modes along its path down the continental slope, and also due to the fact that a large part of the overflow separates from the bottom terrain and flows with neutral buoyancy into the North Atlantic, thus creating an intermediate water mass. This complexity makes the Mediterranean overflow an attractive scientific problem on which to focus.

Modeling can be an important tool for understanding more about the processes involved in marginal sea overflows. Efforts to model and study these overflows were made by several investigators using the so-called 'streamtube model' (see, for example, Smith, 1975; Killworth, 1977; Price and Baringer, 1994; Baringer and Price, 1997). But the 1-dimensionality of the streamtube model makes it limited in many aspects of simulating overflows, such as reproducing the separation of the Mediterranean overflow into different modes. Primitive equation numerical models are therefore necessary for a realistic 3-dimensional approach (Jungclaus and Backhaus, 1994; Gawarkiewicz and Chapman, 1995; Jiang and Garwood, 1995, 1996; Jungclaus and Mellor, 2000). Large-scale ocean models will not resolve the small-scale billows that accomplish the entrainment for the foreseeable future. But increasingly they do resolve the intermediate scale (tens of kilometers in the horizontal) environment which may control the aggregate entrainment, raising the prospects for successful parameterization. Until recently, in isopycnic coordinate models and specifically in the Miami Isopycnic Coordinate Ocean Model (MICOM), the diapycnal exchange of properties has been parameterized using a constant, depth dependent, or buoyancy-frequency-dependent eddy diffusivity. Efforts to model the overflows thus resulted in underestimation of the mixing rates between the overflow water and the ambient water (Willebrand et al., 2001). This poor estimate of the mixing is despite the natural tendency of the vertical resolution in isopycnic models to concentrate at the top of the overflow plume, precisely where the mixing occurs. The prospect for improvement by the inclusion of a Richardson (Ri) number dependent diapycnal mixing scheme, following the Turner (1986) parameterization for entrainment, in a primitive equation numerical ocean model such as MICOM was the principal motivation for this work.

The parameterization of entrainment of ambient water into the overflow involves diapycnal fluxes of mass and momentum and must therefore be realized through the diapycnal mixing

routine. The development of such a Richardson number mixing scheme is not trivial. The governing equations, when discretized using an explicit time integration scheme, have to satisfy a numerical stability criterion such that $\Delta t \leqslant h^2/2K$, where Δt is the time step, K is the diapycnal diffusivity, and h is the layer thickness. Because of this criterion, stability problems are encountered in the limit of vanishing layer thickness and/or large diffusivities, conditions that will undoubtedly arise in an effort to produce a realistic overflow experiment with an isopycnic model incorporating a Richardson number diapycnal mixing scheme.

In order to overcome the limitations created by the stability criterion in explicit schemes, Hallberg (2000) derived an implicit time integration scheme for diapycnal diffusion in isopycnal models. The scheme uses a Newton method iteration to estimate the diapycnal mass flux for a given layer, using an estimate of the derivative of the diapycnal mass flux of the layer with respect to the diapycnal mass fluxes of the neighboring layers. Hallberg (2000) also implemented the entrainment Richardson number parameterization of Turner (1986), together with the diapycnal diffusion mixing scheme, using a semi-implicit approach. Hallberg (2000) showed in a 3-dimensional idealized experiment that this scheme is able to capture the principal characteristics of entraining bottom gravity currents.

In this paper, a series of realistic simulations of the Mediterranean outflow performed with MICOM and the diapycnal mixing scheme of Hallberg (2000) is discussed in detail. The experiments aim to study the behavior of the Mediterranean outflow within the Gulf of Cadiz and near Cape St. Vincent where the Mediterranean undercurrent flows into the open North Atlantic, and to compare the modeled behavior to observations. Sensitivity experiments are also performed with regard to the Richardson number mixing parameterization of Turner (1986) and other model parameters.

2. Background

2.1. Observations of the Mediterranean outflow

Most of the dense water that fills the deep ocean derives from local formation in marginal seas. The dense water overflows at the connecting strait and then flows down the topography and into the ocean interior while mixing with the surrounding water. In the Mediterranean sea, evaporation produces a very dense ($\sigma_\Theta > 28.95$ kg m^{-3}) and saline ($S > 38.4$ psu) source water with temperatures close to 13.0 °C, which overflows at the Strait of Gibraltar into the North Atlantic. This Mediterranean outflow then mixes with relatively fresher (35.6–35.7 psu) and colder (11.4–12.5 °C) North Atlantic Central Water (NACW) (Price and Baringer, 1994) and becomes an intermediate water mass in the North Atlantic. The Mediterranean water that enters the Strait of Gibraltar consists of two different water masses (Kinder and Parilla, 1987), the Levantine Intermediate Water with salinity 38.47–38.49 psu and temperature 13.1–13.2 °C, and the Western Mediterranean Deep Water with salinity 38.42 psu and temperature 12.75 °C . The Mediterranean outflow in the following experiments will be represented by a single water mass with potential density $\sigma_\Theta = 28.94$ kg m^{-3} and salinity $S = 38.4$ psu.

One of the main characteristics of the Mediterranean outflow is the separation of the gravity current into two different cores during its descent down the continental slope and into the Gulf of

Table 1
Review of the properties observed for the upper and lower cores of the Mediterranean outflow by Ambar and Howe (1979) and Baringer and Price (1997), at approximately 7, 8, and 9°W

Section	Lower				Upper			
	S (psu)	Θ (°C)	σ_Θ (kg m^{-3})	Depth (m)	S (psu)	Θ (°C)	σ_Θ (kg m^{-3})	Depth (m)
AH $\sim$ 7°W	37.42	13.16	28.28	756	37.07	13.72	27.88	500–650
BP $\sim$ 7°W	37.21	12.68	28.18	744	36.77	12.79	27.81	672
AH $\sim$ 8°W	36.63	12.28	27.85	1285	36.48	13.05	27.57	700–800
BP $\sim$ 8°W	36.57	11.87	27.83	1204	36.47	12.85	27.56	758
AH $\sim$ 9°W	36.57	12.18	27.83	1315	36.43	13.07	27.52	755
BP $\sim$ 9°W	36.60	11.96	27.84	1366	36.44	12.67	27.58	764

Cadiz. The cause of the separation has been attributed to many different factors. Madelain (1970) suggested that topographic steering could influence the separation process. Seidler (1968) proposed that the discontinuities in the outflow current due to the semi-diurnal tidal mixing at the Strait of Gibraltar could be responsible for formation of the two cores. Ambar and Howe (1979) suggested that the shallower and deeper boundaries of the Mediterranean outflow water mix with the NACW (which differs in temperature and salinity), thus producing an upper core with different properties from those of the main outflow current. This lighter upper core therefore separates from the rest of the outflow simply because its density is more appropriate to lying at shallower depths in the North Atlantic. The properties of the two cores are well documented in Ambar and Howe (1979) and Baringer and Price (1997), as shown in Table 1. The data analyzed by Ambar and Howe (1979) were collected during cruises of the R.R.S. Shackleton (March 1973) and R.R.S. Challenger (August 1976). The data analyzed by Baringer and Price (1997) were collected during the 1988 Gulf of Cadiz Expedition.

The Mediterranean outflow mass transport estimate is also an important issue that has been given much emphasis in the literature. The pure Mediterranean water enters the east end of the Strait of Gibraltar and flows westward, while mixing with the overlying Atlantic inflow water within the Strait, and then exits the west end of the Strait of Gibraltar as the Mediterranean outflow initial water mass. During its descent down the continental slope and into the Gulf of Cadiz, the Mediterranean outflow further mixes with the NACW, therefore increasing substantially [up to three times (Baringer and Price, 1997)] its initial transport by the time it reaches Cape St. Vincent. Several estimates have been made concerning the Mediterranean outflow water mass transports. Baringer and Price (1997) estimate an initial transport of 0.7 Sv (1 Sv = 10^6 m^3 s^{-1}) near the Strait and a transport of 1.9 Sv near Cape St. Vincent. Ambar and Howe (1979) estimate a transport of 1 Sv near the Strait and 1.9 Sv near Cape St. Vincent. Other estimates suggest initial values of the Mediterranean outflow from 0.5–1.8 Sv near the Strait, up to 1.9–3.7 Sv near Cape St. Vincent.

2.2. Meddies

Meddies are coherent anticyclonic-rotating eddies consisting of warm and salty Mediterranean outflow water. After formation, the Mediterranean undercurrent reaches Cape St. Vincent and turns northward, flowing along the Portuguese coast. Part of the undercurrent separates from the

boundary to form meddies that propagate westward. Meddies typically have a diameter between 40 and 150 km, maximum swirl velocities of 50 cm s^{-1}, and maximum salinities of 36.6 psu. These subsurface vortices are found between depths of 600 and 1700 m (Richardson et al., 2000).

The formation mechanism of meddies is not yet fully understood. D'Asaro (1988) argues that the negative relative vorticity in the boundary current, due to viscous shear stress acting in the boundary layer, is responsible for the negative relative vorticity found in meddies. When the current, and thus the boundary layer, separates from the boundary, anticyclonic vortices are formed. Jungclaus (1999), in a series of experiments with a high resolution 3-dimensional primitive equation ocean model, suggests that baroclinic instability of the undercurrent is responsible for meddy formation, although the sensitivity experiments in his study show that topographic irregularities enhance the instability of the undercurrent, thereby favoring the formation of the vortices. Bower et al. (1997), during A Mediterranean Undercurrent Seeding Experiment (AMUSE), deployed floats in the Mediterranean undercurrent to study possible mechanisms of meddy formation. The negative relative vorticity found both in meddies and in the Mediterranean undercurrent led Bower et al. (1997) to the conclusion that the theory of D'Asaro (1988) is the most likely principal meddy formation mechanism. Stern and Chassignet (2000) show that the classical finite amplitude instability theory in boundary currents is not sufficient to explain eddy separation. They claim that the separation requires an additional process such as a downstream velocity convergence created by topographic features or fluctuations at the source of the undercurrent. The latter source of downstream velocity convergence, in the case of the Mediterranean outflow, could result from the influence of tides at the Strait of Gibraltar, which often completely reverse the direction of the outflow at the Strait.

3. Model description and configuration

The numerical experiments were carried out with the MICOM. MICOM is well documented in the literature (see Bleck et al. (1992) and Bleck and Chassignet (1994) for details).

The computational domain includes the Gulf of Cadiz and a small portion of the eastern North Atlantic Ocean basin. The longitude ranges from 5.92°W, on the west end of the Strait of Gibraltar at the top of the Spartell Sill, to 13.52°W in the North Atlantic. In latitude, the basin extends from 34.44 to 40.7°N. The horizontal resolution is 1/12°, as adopted by Chassignet and Garraffo (2001) for a fine-mesh simulation of the North and Equatorial Atlantic. The model grid consists of 100 points in the north-south direction and 96 in the west–east direction. The bottom topography (Fig. 1) is derived from a digital terrain data set with 2.5′ latitude–longitude resolution (ETOPO2.5). The vertical structure is defined by 27 isopycnic layers, with potential density [σ_Θ (kg m^{-3})] values of 25.77, 26.18, 26.52, 26.80, 27.03, 27.10, 27.15, 27.20, 27.26, 27.32, 27.38, 27.44, 27.50, 27.55, 27.60, 27.64, 27.70, 27.74, 27.82, 27.88, 27.92, 28.00, 28.10, 28.30, 28.50, 28.70, and 28.94. The initial mass field is based on the Levitus (1982) June climatology for temperature and salinity. The model was spun up from rest for 1 year. Since the primary focus of this work is to evaluate the impact of the entrainment parameterization on the Mediterranean outflow, no atmospheric forcing was included in the model.

The Mediterranean outflow is forced as a source on the eastern boundary of the model at the western end of the Strait of Gibraltar. At 6°W, the zonal velocities, salinities, and layer interface
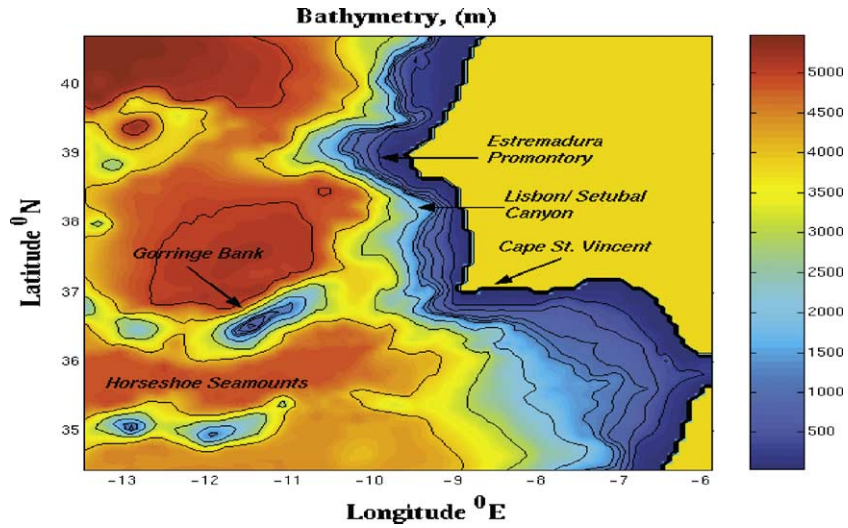
Fig. 1. Model bathymetry of the Gulf of Cadiz and the Eastern North Atlantic Ocean Basin.

depths that define the water mass exchange between the Mediterranean Sea and the Atlantic are prescribed at all times (see Fig. 2 for details). At the source, the Mediterranean outflow lies solidly in the bottom layer with potential density 28.94 kg m^{-3} and salinity 38.4 psu, and its transport is set to a constant value of 0.8 Sv (Baschek et al., 2001) by specifying a constant zonal velocity equal
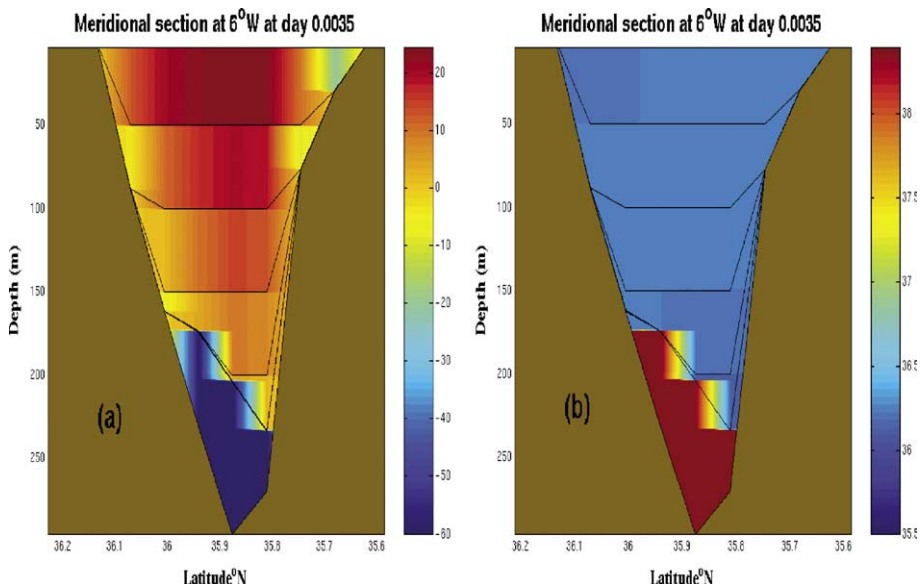

Fig. 2. Vertical profile of layer thickness at meridional section 6°W showing the Mediterranean outflow and inflow forcing in the eastern boundary of the model. (a) Color contours represent layer zonal velocities (cm s^{-1}). Positive values indicate flow to the east. (b) Color contours represent layer salinities (psu).

to 60 cm S^{-1}. The inflow transport of Atlantic Water to the Mediterranean Sea is also set to 0.8 Sv. The slope of the interface between the outflow and the overlying water was estimated from geostrophy.

The northern, southern, and western boundaries are open (zonal and meridional velocities are non-zero at the boundaries throughout the simulation) with a sponge layer 2/3° wide in which salinity and layer interface depths are relaxed to their initial Levitus values and velocities are damped to zero. The restoring time scales vary from 10 min to 5 h, from the inner to the outer edges of the buffer zone. Finally, entrainment is parameterized following Turner (1986) using the Hallberg (2000) diapycnal mixing scheme. The background diapycnal diffusion coefficient is set to the traditional 1 cm^2 s^{-1}.

The parameters of the various experiments are described below and are summarized in Table 2. All experiments are performed in the basic configuration outlined above unless otherwise stated. Sensitivity experiments are carried out regarding the Richardson number turbulent mixing parameterization, the properties of the Mediterranean outflow at the west end of the Strait of Gibraltar, and the diapycnal mixing frequency coefficient (which controls the time elapsed between subsequent activations of the diapycnal mixing scheme in the model).

The first experiment A1, is performed with the Richardson number entrainment parameterization given by Turner (1986),

$$E1 = \begin{cases} \Delta U \frac{0.08-0.1Ri}{1+5Ri}, & Ri < 0.8, \\ 0, & Ri \geqslant 0.8, \end{cases} \tag{1}$$

where ΔU is the magnitude of the velocity difference between the outflow and the ambient water and Ri is the layer Richardson number for the outflow. (Note that with Turner's definition of the Richardson number, $Ri = 1$ is the critical value for the development of inviscid Kelvin–Helmholtz instabilities.) The diapycnal mixing is equal to 1 and the Mediterranean outflow zonal velocity is equal to 60 cm s^{-1} with a constant outflow transport of 0.8 Sv. In Experiment A1*, the set-up is identical to A1 except that the value of the diapycnal mixing frequency is set to 1/144, corresponding to an interval of 0.5 days (the baroclinic time step is 300 s).

The entrainment parameterization E1 of Turner (1986) in Eq. (1) was derived from a series of idealized laboratory experiments and may not be applicable to oceanic gravity currents, due to the

Table 2
Description of the model experiments

Experiments	Entr. param.	mixfrq	Vel. (cm s^{-1})	Trans. (Sv)	Pot. dens (kg/m^3)	Saln. (psu)
A1	E1	1	60	0.8	28.94	38.4
A1*		1/144				
A2	E2	1				
A3	E3					
A4	E4					
A5	E5					
A6	E1				28.40	37.8
A7		1/144	0–120	0–1.6	28.94	38.4
A8		1				

Blanks indicate no change from the previous experiment.

use of a bulk Richardson number instead of a shear Richardson number and the absence of rotation. Experiments with different entrainment parameterizations are therefore performed in order to test the sensitivity of the Mediterranean outflow properties (including meddy formation) to the magnitude of mixing with NACW. The four experiments A2, A3, A4, and A5 are performed with the following Richardson number entrainment parameterizations respectively,

$$E2 = \begin{cases} \Delta U \frac{0.07-0.1Ri}{1+5Ri}, & Ri < 0.7, \\ 0, & Ri \geqslant 0.7, \end{cases}$$

$$E3 = \begin{cases} \Delta U \frac{0.09-0.1Ri}{1+5Ri}, & Ri < 0.9, \\ 0, & Ri \geqslant 0.9, \end{cases}$$

$$E4 = \begin{cases} \Delta U \frac{0.09-0.1Ri}{1+5Ri}, & Ri < 0.7, \\ 0, & Ri \geqslant 0.7, \end{cases} \tag{2}$$

$$E5 = \begin{cases} \Delta U \frac{0.12-0.1Ri}{0.6+3Ri}, & Ri < 0.9, \\ 0, & Ri \geqslant 0.9. \end{cases}$$

The entrainment mixing parameterizations (E1–E5) are plotted against the Richardson number in Fig. 3. The basic form of the entrainment parameterization of Turner (1986) was not changed when specifying E2 and E3. Only the constant coefficients of the Richardson number inside the equation were altered, aiming to decrease/increase the entrainment velocity. Experiment A2 performed with E2 aims to produce less mixing of the Mediterranean outflow with the NACW, together with a lower value for the critical *Ri* number (0.7). Experiment A3 performed with E3 aims to produce more mixing together with a higher value for the critical *Ri* number (0.9). Experiment A4 performed with E4 [Same critical *Ri* number (0.7) as A2 and same entrainment rate
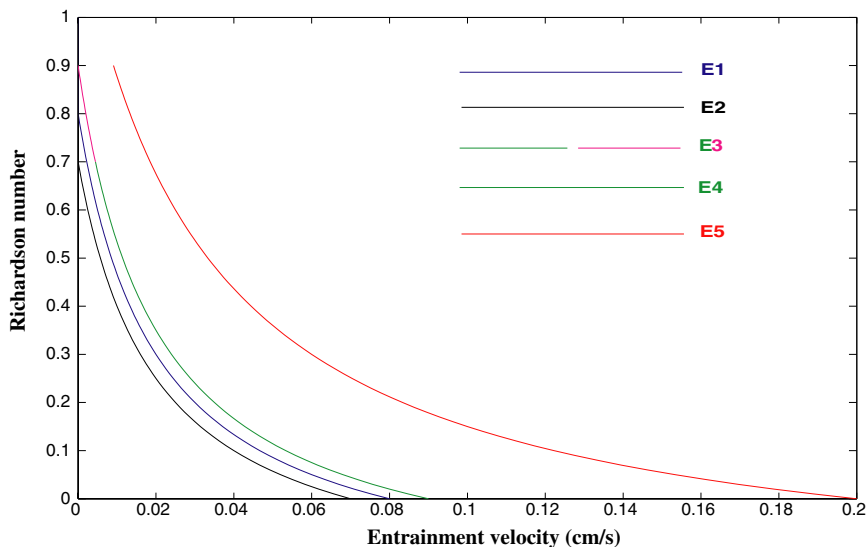
Fig. 3. Comparison of the mixing rates in the various experiments. Entrainment velocities E1–E5 are plotted against the Richardson number in Eqs. (1) and (2). ΔU is chosen to be $1\ \mathrm{m\,s^{-1}}$.

as A3] aims to investigate the importance of the entrainment parameterization versus that of the critical *Ri* number in the mixing of the Mediterranean outflow with NACW. Entrainment parameterization E5 in experiment A5 aims to produce a very high mixing rate between the ambient water and the Mediterranean outflow. Experiments A1, A2, A3, A4, and A5 are performed with diapycnal mixing frequency equal to 1, a constant Mediterranean outflow zonal initial velocity of 60 cm s^{-1}, and a constant initial outflow transport of 0.8 Sv.

Experiment A6 uses the same set-up as A1 with the initial Mediterranean outflow potential density and salinity at the source chosen to be 28.40 kg m^{-3} and 37.8 psu respectively. The experiment aims to test the sensitivity of the properties of the outflow downstream to the initial properties of the outflow at the source. In A6, the outflow is more buoyant and fresher than in the previous experiments.

Finally, experiments A7 and A8 are performed with entrainment parameterization E1 and diapycnal mixing frequencies equal to 1/144 and 1, respectively, but with the outflow initial velocity at the source varying sinusoidally between 0 and 1.2 m s^{-1} with a period of half a day. The outflow transport varies proportionally (0–1.6 Sv and back to 0) to the velocity, with the outflow interface at the Strait kept constant at all times. This outflow behavior resembles the realistic outflow scenario when influenced by the semi-diurnal tide at the Strait. The outflow interface is not adjusted geostrophically with the varying velocity at all times but rather kept identical to the constant initial geostrophically adjusted interface corresponding to the 60 cm s^{-1} outflow velocity. This assumption can be justified by the fact that the inertial period at the Strait, ∼0.9 days, is larger than (almost double) the tidal period, ∼0.5 days.

4. Results of model experiments

In this section, the results of experiments A1–A8 are described. The characteristics of the modeled Mediterranean outflow, such as its properties, mass transport, path within the Gulf of Cadiz and into the North Atlantic, and associated meddy formation are investigated in each of the experiments and compared to observations.

4.1. The base experiment A1

As described in Section 3, the Mediterranean outflow is initialized at the western end of the Strait of Gibraltar at 6°W, as a source of mass with potential density (σ_{Θ}) 28.94 kg m^{-3}, salinity (*S*) 38.4 psu, and zonal velocity 60 cm s^{-1}. The outflow traverses and descends the continental slope while mixing with the overlying NACW. Fig. 4 shows a meridional section at 6.88°W of layer thicknesses, velocities, and salinities after 200 days of simulation of experiment A1. The mixing of the outflow with ambient water is evident from Fig. 4. The outflow salinity observed at section 6.88°W lies between 36.4 and 37.2 psu with maximum outflow velocity of 45 cm s^{-1}. The average outflow thickness is approximately 200 m and the width is 60 km. The onshore depth of the outflow is 450 m and the offshore depth 750 m.

The outflow lies between layers 14 and 20, which correspond to potential densities of 27.55–27.88 kg m^{-3}. These values of outflow characteristics agree (with a considerable degree of accuracy) with observations made by Baringer and Price (1997). At station F (∼7°W), in the 1988
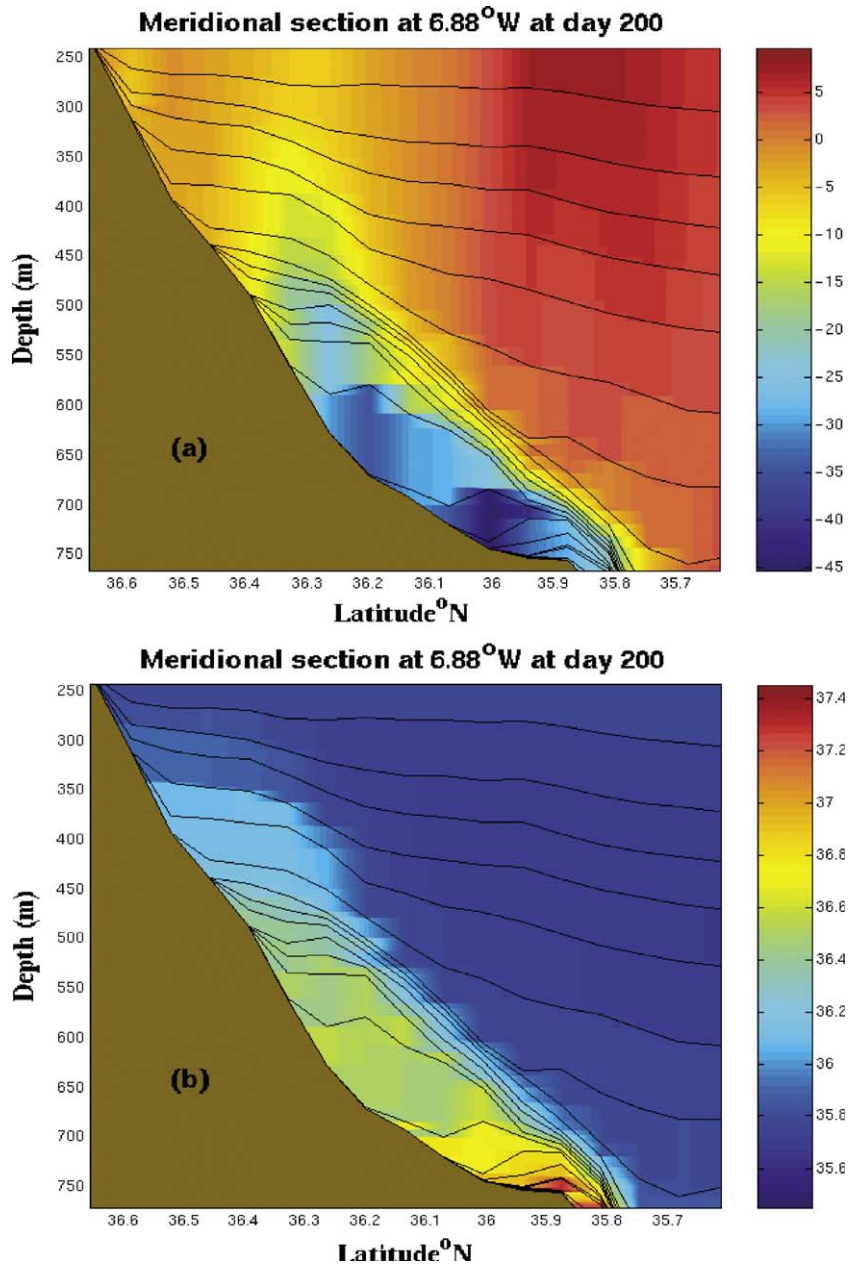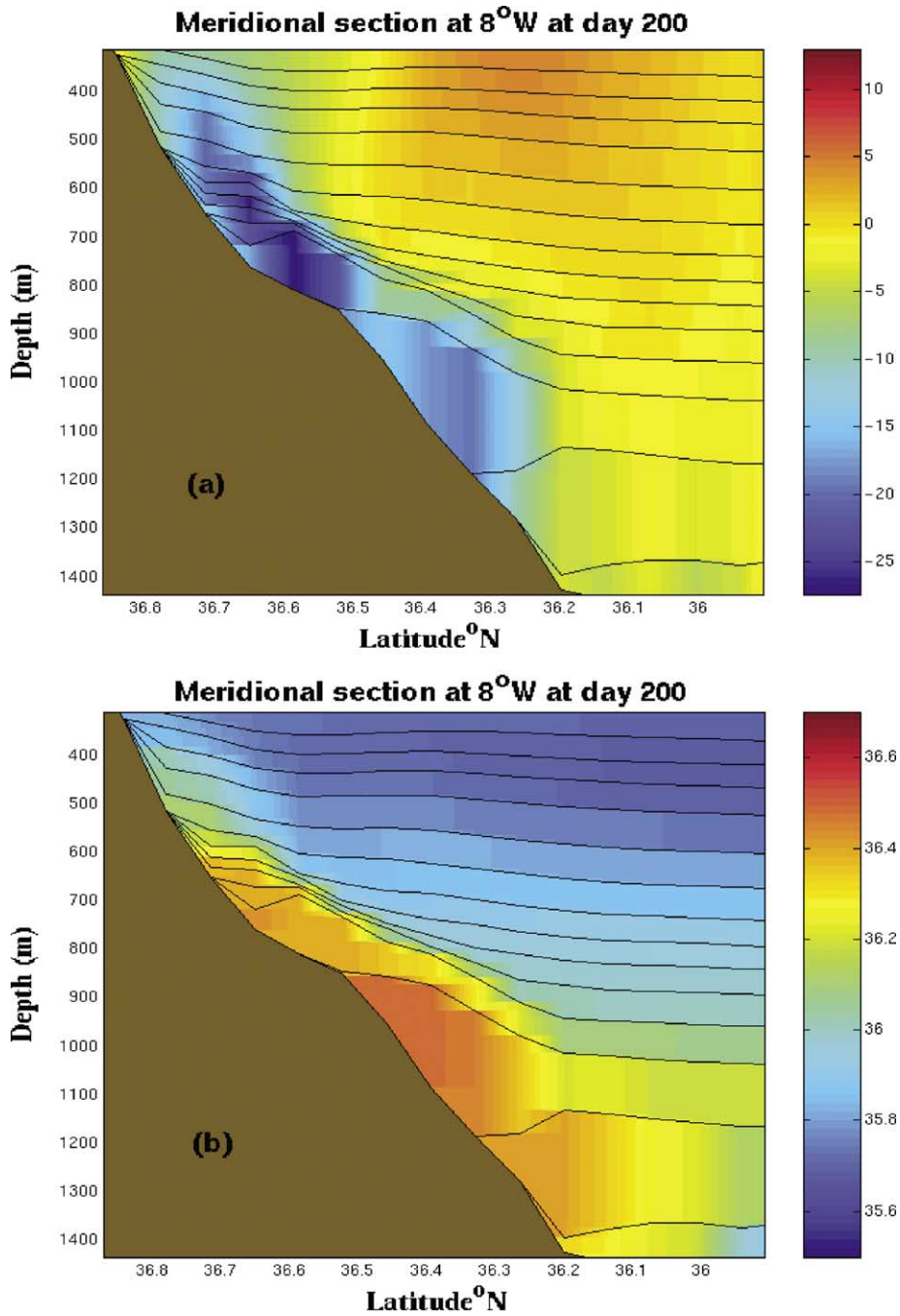
Fig. 4. Vertical profile of layer thickness at meridional section 6.88°W at day 200 in experiment A1. (a) Color contours represent layer zonal velocities (cm s^{-1}). Positive values indicate flow to the east. (b) Color contours represent layer salinities (psu). The Mediterranean undercurrent mixes with the ambient NACW while flowing down the continental slope.

Gibraltar Experiment, Baringer and Price (1997) observed the Mediterranean outflow between depths of 400 and 800 m, with salinities between 36.5 and 37.21 psu, maximum velocities of

Fig. 5. Vertical profile of layer thickness at meridional section 8°W at day 200 in experiment A1. (a) Color contours represent layer zonal velocities (cm s^{-1}). Positive values indicate flow to the east. (b) Color contours represent layer salinities (psu).
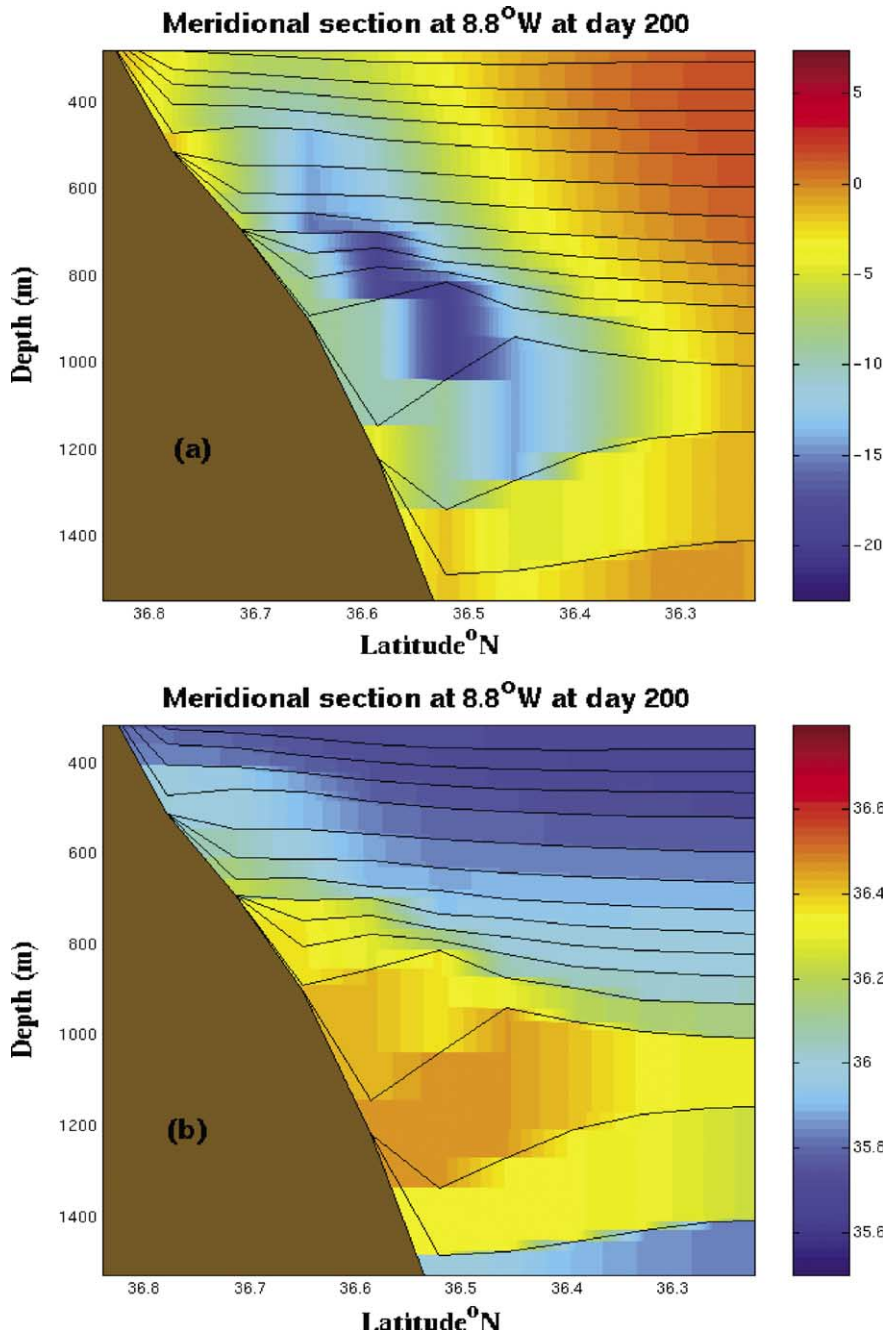
Fig. 6. Vertical profile of layer thickness at meridional section 8.8°W at day 200 in experiment A1. (a) Color contours represent layer zonal velocities (cm s^{-1}. Positive values indicate flow to the east. (b) Color contours represent layer salinities (psu). The Mediterranean undercurrent settles at a constant depth between 450 and 1300 m near the tip of Cape St. Vincent.

50 cm s^{-1}, and potential densities of 27.50–28.18 kg m^{-3}. At section 8°W (Fig. 5), the modeled outflow lies between depths of 500 and 1300 m in layers 13–20 with potential densities 27.50–27.88 kg m^{-3} and salinity between 36.2 and 36.6 psu. The maximum velocity is 27 cm s^{-1}. Those results at section 8°W are also in agreement with observations. Baringer and Price (1997) observed the Mediterranean outflow at section H (∼8°W) between 450 and 1300 m, with potential densities between ∼27.56 and 27.83 kg m^{-3} and salinities between 36.00 and 36.57 psu. Fig. 6 illustrates the modeled Mediterranean outflow at section 8.8°W, at the tip of Cape St. Vincent, between depths of 500 and 1400 m, with potential densities of 27.38–27.82 kg m^{-3} and salinities from 36.1–36.5 psu. The maximum outflow velocity is 23 cm s^{-1}. The results of experiment A1 at the various sections are summarized in Table 3.

The initial Mediterranean outflow transport is increased due to mixing with the NACW from 0.8 Sv at section 5.92°W to 1.66 Sv at section 6.88°W (Fig. 7). Farther down the continental slope, the outflow transport increases to 2.3 Sv at section 8°W. The mixing rate of the Mediterranean outflow with the NACW decreases further west, and the outflow transport at Cape St. Vincent (section 8.8°W) is found to be 2.42 Sv. Thus, the modeled Mediterranean outflow transport increases to approximately three times its initial value until it reaches Cape St. Vincent, in good agreement with estimates and observations found in the literature (Baringer and Price, 1997). The transport values of the Mediterranean outflow given in this paragraph and hereafter are outflow salinity transports, defined as the transport of Mediterranean outflow water flowing westward with salinities higher than the salinities of the surrounding Atlantic water. Note that the choice of minimum salinity for calculating transports varies at the different sections of the path of the outflow, depending on the salinities of the Mediterranean outflow and the surrounding Atlantic water at the particular section. In experiment A1, the Mediterranean outflow shows no evidence of separation into different cores. Although the mixing with overlying NACW and the path of the outflow produce different velocity and salinity characteristics in the onshore and offshore parts of the outflow, as seen in Fig. 5, the outflow lies primarily in layers 17 and 18 at all times up to reaching Cape St. Vincent (Fig. 7) and behaves as a single core. After passing Cape St. Vincent, the outflow separates from the bottom and flows as an intermediate water mass into the North Atlantic; proceeding northward along the

Table 3
Mediterranean outflow properties in experiments A1, A2, A3, and A4 at sections 6.88, 8, and 8.8°W after 200 days of simulation

| Exps/secns	S (psu)	σ_Θ (kg m^{-3})	Depth (m)	Max. vel (cm/s)	Trans (Sv)
A1-6.88°W	36.4–37.2	27.55–27.88	450–750	45	1.66
A2-6.88°W	36.4–37.4	27.60–27.88	450–750	45	1.52
A3-6.88°W	36.3–37	27.50–27.88	400–750	39	1.97
A4-6.88°W	36.35–37.1	27.50–27.88	450–750	39	1.9
A1-8°W	36.2–36.6	27.50–27.88	500–1300	27	2.3
A2-8°W	36.2–36.7	27.50–27.88	550–1300	26	2.15
A3-8°W	36.2–36.45	27.44–27.88	500–1250	27	2.42
A4-8°W	36.25–36.6	27.50–27.88	500–1300	26	2.2
A1-8.8°W	36.1–36.5	27.38–27.82	500–1400	23	2.42
A2-8.8°W	36.1–36.55	27.44–27.82	550–1400	21	2.25
A3-8.8°W	36.1–36.4	27.38–27.82	400–1250	20	2.53
A4-8.8°W	36.1–36.53	27.44–27.82	550–1350	20	2.29
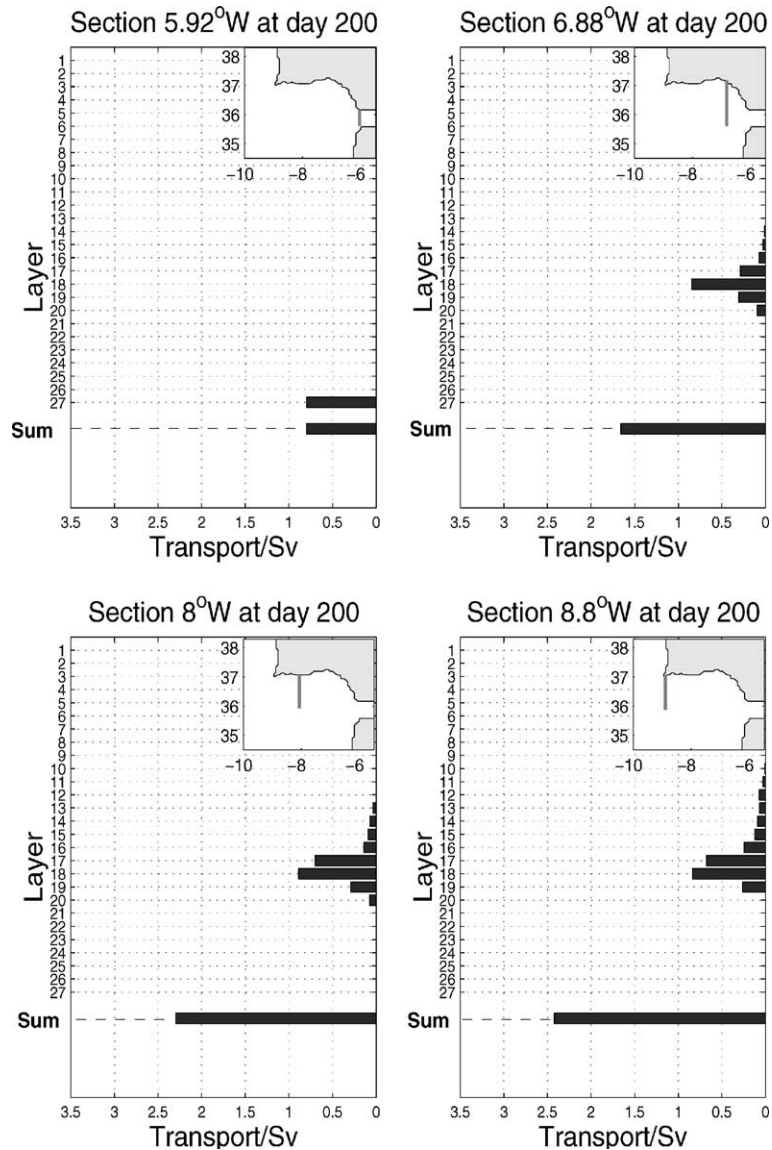
Fig. 7. Mediterranean outflow transport in isopycnic layers at meridional sections 5.92, 6.88, 8, and 8.8°W at day 200 in experiment A1.

Portuguese coast (Fig. 8). Fig. 9 shows the horizontal salinity distribution at day 200 for layers 16, 17, and 18. Note that the Mediterranean undercurrent has detached from the bottom while flowing north along the Portugal as an intermediate water mass, as seen in Fig. 10.

The similarity of the model results to observations in the region (listed in Table 1) confirms that, in a realistic configuration, one can correctly simulate the behavior of entraining bottom gravity currents and successfully capture their main characteristics by using Turner (1986) entrainment parameterization. In the absence of any entrainment parameterization in the model,

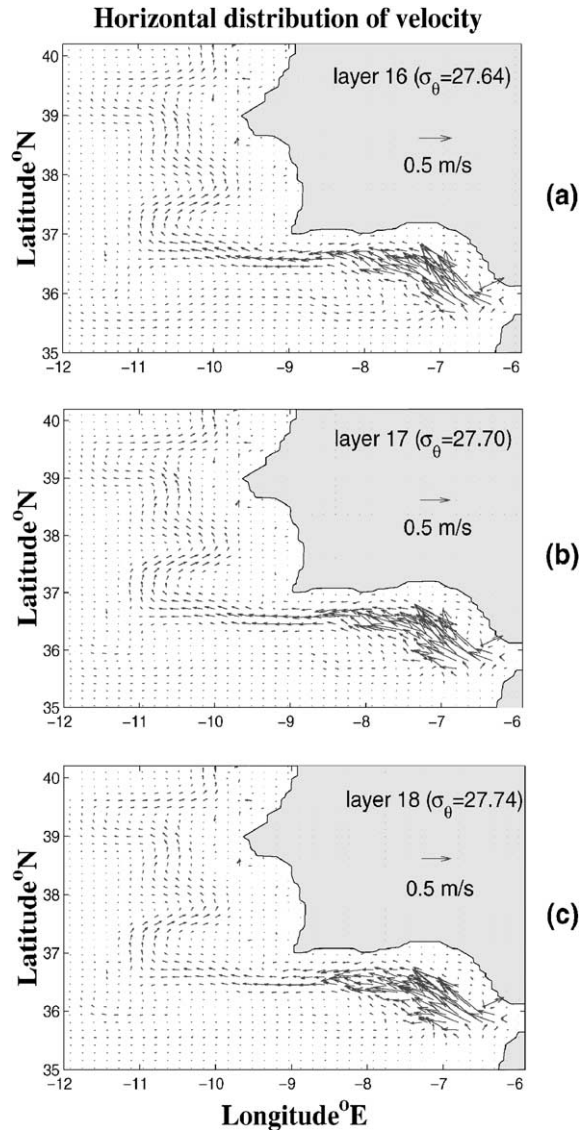## Horizontal distribution of velocity

Fig. 8. Horizontal distribution of velocity at day 200 in isopycnic layers 16, 17, and 18 in experiment A1. The figure shows the path of the Mediterranean outflow into the North Atlantic.

the Mediterranean outflow water would remain in the bottom layer without mixing with the ambient water and flow into the North Atlantic ultimately flooding the abyss. The outcome differs little if a constant diffusivity with values appropriate to the interior is used.

4.2. Sensitivity to entrainment parameterization

Section 4.1 showed that MICOM with the Turner (1986) entrainment parameterization scheme is able to model a Mediterranean outflow with characteristics that are in agreement with

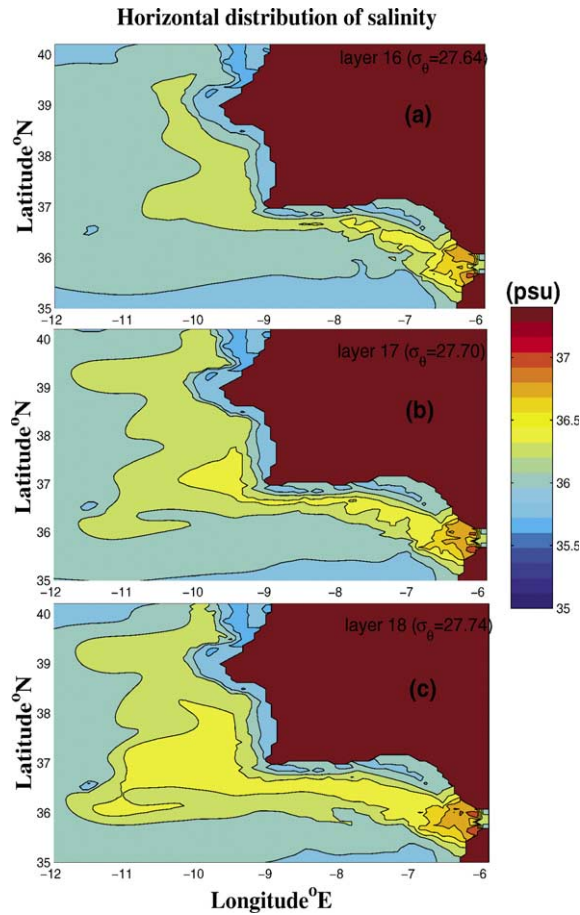**Horizontal distribution of salinity**

Fig. 9. Horizontal distribution of salinity at day 200 in isopycnic layers 16, 17, and 18 in experiment A1.

observations. It is important, however, to investigate the sensitivity of these results to certain parameters within the entrainment parameterization. Experiments A2, A3, and A4 are therefore performed with the entrainment parameterizations E2, E3, and E4, respectively, as shown in (2) and discussed in Section 3. The results of these three experiments are summarized in Table 3. As expected, A2 produces less mixing than A1 between the Mediterranean outflow and the overlying NACW during the outflow descent down the continental slope within the Gulf of Cadiz. The salinity characteristics of the outflow in A2 in sections 6.88, 8, and 8.8°W show similar values for the outflow salinity minimum as that of A1, but a higher salinity maximum as an indication of decreased mixing. The outflow also lies deeper on the continental slope. The decreased mixing of the outflow with the NACW in A2 is evident from the transport estimates at the various sections. The Mediterranean outflow transport in A2 at section 8.8°W near Cape St. Vincent, just before it detaches from the bottom to flow neutrally buoyant into the North Atlantic, is estimated to be 0.17 Sv less than the outflow transport estimated in A1.
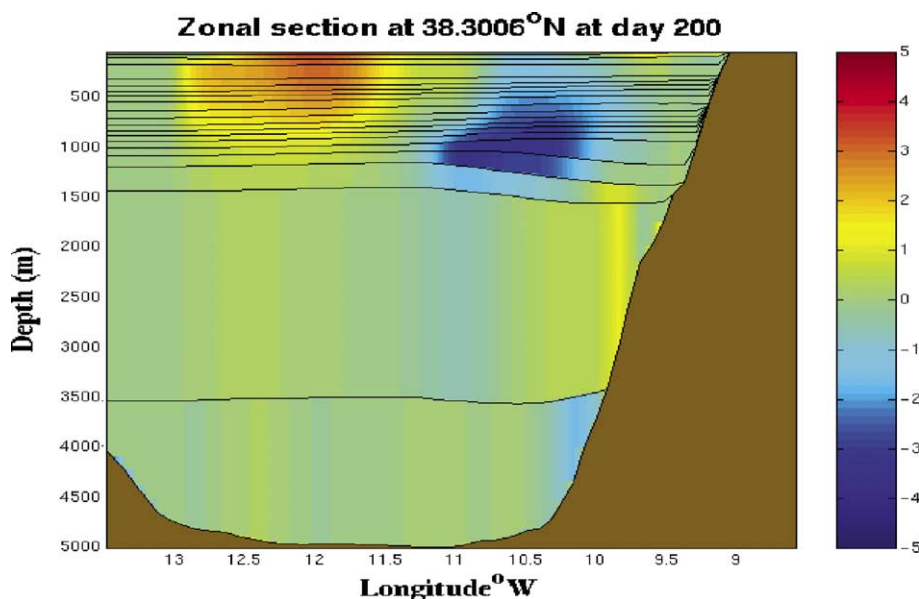
Fig. 10. Vertical profile of layer thickness at zonal section 38.3°N at day 200 in experiment A1. Color contours represent layer meridional velocities (cm s^{-1}). Positive values indicate flow to the south. Note that the Mediterranean undercurrent has detached from the bottom.

Experiment A3, using the stronger entrainment parameterization E3, produces the opposite effects from those seen in A2. The Mediterranean outflow appears to have mixed more with the NACW than in A1, with lower values of maximum salinity and a more buoyant current lying at shallower depths. Transport estimates at the different sections verify the greater mixing in A3, with the Mediterranean outflow at Cape St. Vincent found to have an increased transport of 0.11 Sv compared to that in A1. The results obtained from experiments A2 and A3 indicate that the Mediterranean outflow characteristics are sensitive to the mixing parameterization of ambient water into the bottom gravity current.

Experiment A4, performed with entrainment parameterization E4, aims to investigate the importance of entrainment rates versus the critical Richardson number in the Turner (1986) entrainment parameterization, when compared to A2 and A3. Experiment A4 produces less mixing between the Mediterranean outflow and the overlying NACW than seen in A3 with entrainment parameterization E3. This is not surprising since the value of the critical Ri was reduced from 0.9 in E3 to 0.7 in E4, with both experiments using the same formulation for the entrainment velocity parameterization, i.e., the same entrainment rates. Note also that the rate of increase of the Mediterranean outflow transport in A3 and A4 is similar near the Gibraltar Strait, where the Ri values are less than 0.7. At section 6.88°W, the Mediterranean outflow transport has increased to 246% of its initial value for A3 and to 238% of its initial value for A4. Farther away from the Strait, where the Ri values are close to the critical values (0.7), the rate of increase of the Mediterranean outflow transport drops faster in experiment A4 than in A3. Between sections at 6.88 and 8°W, entrainment occurs less vigorously but is still substantially larger in A3 than in A4 (0.45 Sv versus 0.3 Sv). The comparison between experiments A4 and A3 illustrates how sensitive the

modeled Mediterranean outflow properties are to the choice of a critical Richardson number, particularly in the later evolution of the plume.

Experiment A4 has the same critical Ri (0.7) as A2, but with larger entrainment velocities and hence larger entrainment rates. At section 6.88°W, the Mediterranean outflow transport of A2 is calculated to be 1.52 Sv in comparison with the 1.9 Sv of A4, due to the higher entrainment rates given by E4 in comparison to E2. Between sections 6.88 and 8.8°W, however, the Mediterranean outflow transport for A2 increases by 0.63 to 2.15 Sv in comparison to the 0.3 Sv increase to 2.2 Sv in A4. Noting the maximum velocities at section 6.88°W in Table 3, it can be seen that the stronger mixing in A4 compared to that in A2 slows down the Mediterranean undercurrent to 39 cm s^{-1} in A4 (as compared to 45 cm s^{-1} in A2) by the time it reaches 6.88°W. Therefore, between sections 6.88 and 8°W, higher velocities in experiment A2 produce lower values of Ri than in experiment A4, and more mixing is produced in A2 than in A4 despite the higher entrainment rate in E4. Farther downstream, between sections 8 and 8.8°W, the Mediterranean outflow transports of A2 and A4 become almost equal, 2.25 and 2.29 Sv respectively. Overall, experiments A3 and A4 show that, for a given critical Richardson number, the downstream Mediterranean outflow properties are not strongly influenced by the choice of entrainment rate. Initially and close to the Gibraltar Strait, the rate of increase in A4 is much higher than in A2, but the opposite holds downstream. This is reminiscent of the findings of Yu and Schopf (1997) that shear-driven mixing in the equatorial undercurrent is much more sensitive to the threshold for vigorous entrainment than to details of the exact rates.

4.3. Sensitivity to diapycnal mixing frequency

For a constant vertical diffusivity, the diapycnal algorithm performance is independent of the time step or the diapycnal mixing frequency choice as long as it is within the diffusive time scale. Primarily in order to save computer time, this prompted us to experiment with the diapycnal mixing frequency. However, the modeled outflow, and especially the meddy formation process, was found to be quite sensitive to the choice of diapycnal mixing frequency. Experiment A1* is therefore similar to A1, the difference being the use in A1* of a diapycnal mixing frequency of 1/144 (corresponding to a period of 0.5 days) instead of 1 (an interval of 300 s) in A1. Assuming an average velocity of the Mediterranean outflow within the Gulf of Cadiz of 40 cm s^{-1}, ~10 days are required for the outflow to travel from the Strait of Gibraltar to Cape St. Vincent. In A1*, the diapycnal mixing scheme is therefore activated only about 20 times (versus 2880 times in A1) during the time it takes the outflow to traverse this region, in which much of the Mediterranean outflow mixing with the NACW occurs. The infrequent mixing of outflow water in A1* produces higher outflow velocities than in A1, since the bottom gravity current is left undiluted for a substantially longer time, during which it can accelerate down the continental slope. The resulting higher Mediterranean outflow velocities produce smaller Richardson numbers and overall higher turbulent entrainment velocities in experiment A1* than in A1, resulting in more mixing between the Mediterranean outflow and the NACW.

The properties of the outflow at section 8.8°W near Cape St. Vincent for experiment A1* are illustrated in Fig. 11 (and in Fig. 6 for A1). At day 200, the outflow lies between salinities of 36.1–36.6 psu with a maximum velocity of 22 cm s^{-1} in A1*. It is located between isopycnal layers 9–18 (potential densities of 27.26–27.74 kg m^{-3}) and between depths of 500 and 1200 m. The outflow in

Meridional section at 8.8°W at day 200

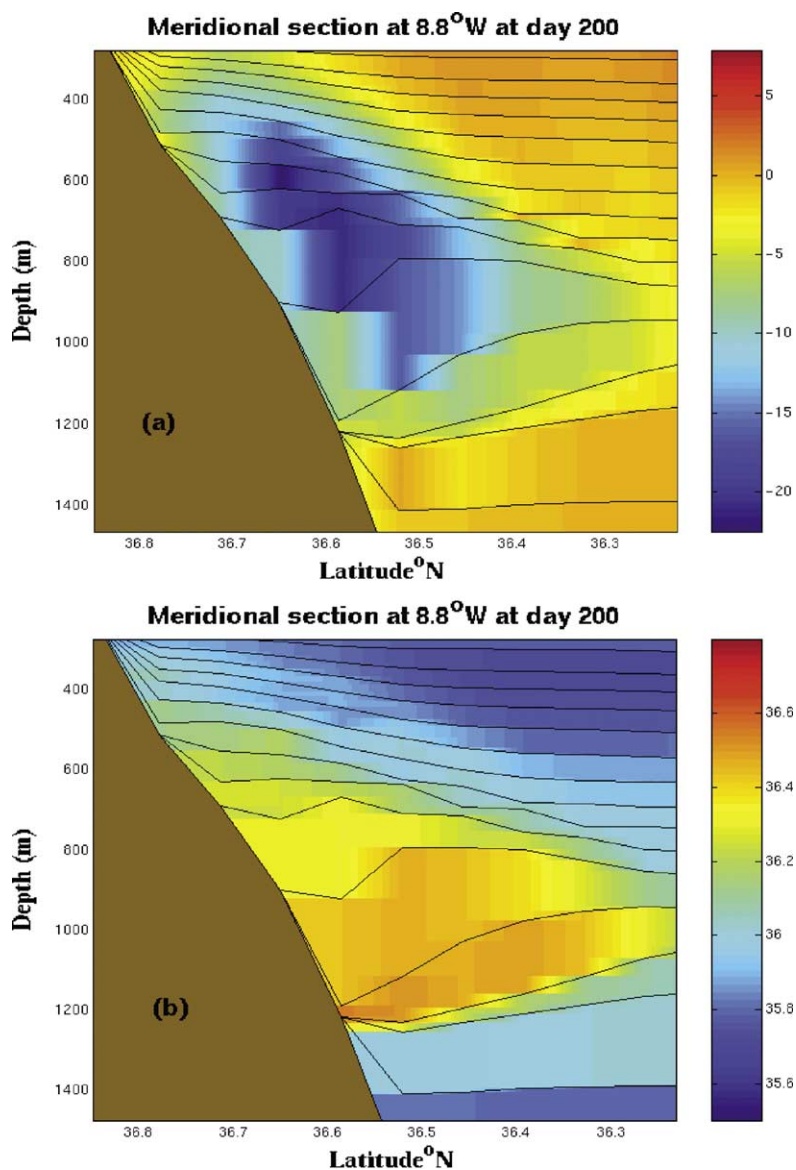
Meridional section at 8.8°W at day 200

Fig. 11. Vertical profile of layer thickness at meridional section 8.8°W at day 200 in experiment A1*. (a) Color contours represent layer zonal velocities (cm s^{-1}). Positive values indicate flow to the east. (b) Color contours represent layer salinities (psu).

A1* is more buoyant and 200 m shallower than that in A1, an indication of the increased mixing of the outflow with NACW in A1*. The mixing increase in A1* can also be seen from Mediter-ranean transport estimates. Fig. 12 illustrates the outflow transports in sections 5.92, 6.88, 8, and 8.8°W. The transport increases from 0.8 Sv at 5.92°W to 1.95 Sv at 6.88°W. By the time the outflow reaches 8°W, the transport in A1* has already increased to 3 Sv, and then to 3.2 Sv at 8.8°W, roughly 30% stronger than in A1.
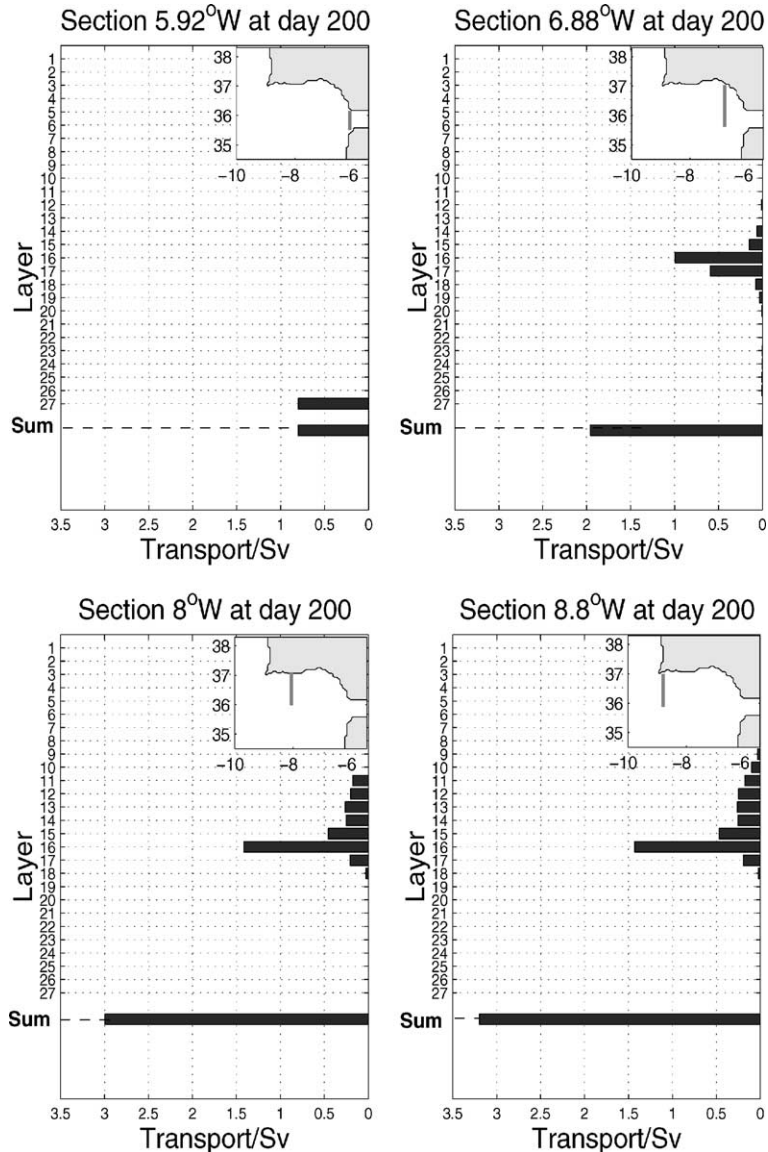
Fig. 12. Mediterranean outflow transport in isopycnic layers at meridional sections 5.92, 6.88, 8, and 8.8°W at day 200 in experiment A1*.

Although the outflow in A1* has mixed more with the NACW than that in A1, the onshore upper part of the A1* outflow is found to be heavier than the ambient water at section 8.8°W, as seen in Fig. 11. This is not the case in A1. The flat isopycnals between the bottom lying undercurrent and the ambient water, illustrated in Fig. 6, indicate that the upper part of the outflow has the same buoyancy as the ambient water. The result is that the upper part of the outflow in A1 does not follow the bottom topography contours and thus does not turn northward at the corner of Cape St. Vincent, but continues to flow west with the rest of the outflow as a single core
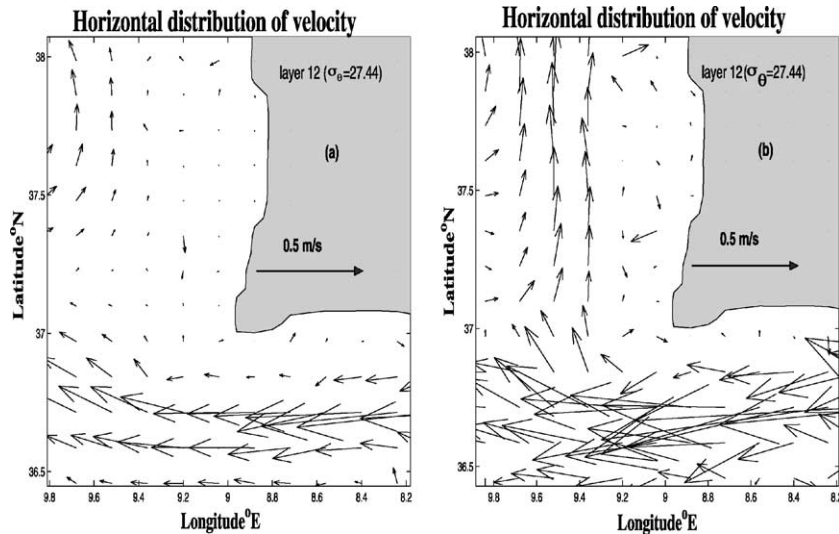
Fig. 13. Horizontal distribution of velocity at day 200 in layer 12. (a) Experiment A1, (b) Experiment A1*. The separation of the Mediterranean outflow into two cores in experiment A1* is evident in (b).

intermediate water mass into the North Atlantic. In A1*, however, the outflow separates into two cores at the corner of Cape St. Vincent. The upper core flows northward on the bottom terrain along the Portuguese coast, and the lower core detaches from the bottom and flows neutrally buoyant into the North Atlantic. Fig. 13 shows the horizontal velocity distribution in layer 12 at day 200 near Cape St. Vincent for experiments A1* and A1. The separation of the outflow in experiment A1* is evident from the velocity contours in Fig. 13b. This will be shown to have an impact on the meddy formation process (Section 4.4).

The fact that the diapycnal mixing frequency in experiment A1* (0.5 days) coincides with half the inertial period (~0.45 days) in the Gulf of Cadiz could account for the increased mixing in A1*, since the largest velocities (and therefore shears) of a current undergoing geostrophic adjustment occur after half of an inertial period. Additional experiments in which the mixing occurs every 2–10 timesteps do not show such a dramatic impact of the mixing frequency (Stephens, personal communication). Further investigation of the importance of the diapycnal mixing frequency value on the entrainment parameterization is needed for a complete understanding of its importance.

4.4. Meddy formation

Experiments A1, A2, A3, and A4 show no evidence of meddy formation throughout 200 days of simulation. In all of these experiments, the Mediterranean outflow detaches from the bottom at Cape St. Vincent and flows neutrally buoyant into the North Atlantic, taking a northward direction along the Portuguese coast as an intermediate water mass. During its northward course, the Mediterranean undercurrent meanders east and west, driven by the influence of bottom topography, specifically the Lisbon/Setubal Canyon and the Estremadura Promontory. At

approximately 38.7°N, the undercurrent actually collides with the Estremadura Promontory, swerves around it, and continues flowing to the north.

Experiment A1*, on the other hand, shows high meddy activity in the region. Fig. 14 illustrates horizontal velocities for layer 15 ($\sigma_\Theta = 27.60 \text{ kg m}^{-3}$) at days 70, 130, 200, and 300. After 70 days

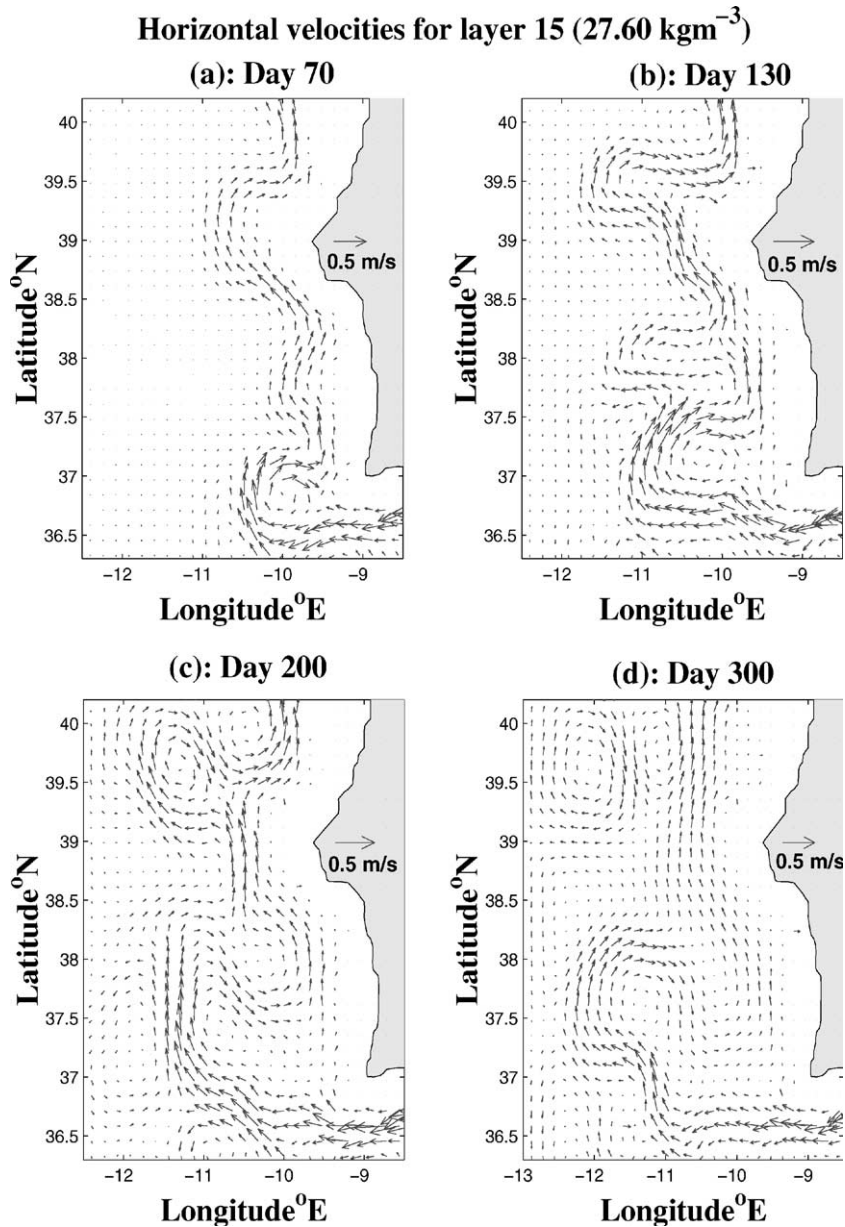**Horizontal velocities for layer 15 (27.60 kgm^{-3})**

Fig. 14. Horizontal distribution of velocity in layer 15 ($\sigma_\Theta = 27.60 \text{ kg m}^{-3}$) at days 70, 130, 200, and 300 in experiment A1*. Meddies tend to form near key topographic features such as the Cape of St. Vincent, the Estremadura Promontory, and the Lisbon/Setubal Canyon.

of simulation, the Mediterranean undercurrent starts to show evidence of meddy formation at the corner of Cape St. Vincent, where the undercurrent separates from the bottom. After 130 days of simulation, there is evidence of three meddies forming in the region, one at the corner of Cape St. Vincent, another in the vicinity of the Lisbon/Setubal Canyon at 38°N, and the other past the Estremadura Promontory at 39.5°N. At day 200, the meddy at the Estremadura Promontory begins to separate. The meddy-like feature at the corner of Cape St. Vincent does not move farther to the west from the region, nor does it show any evidence of detaching from the undercurrent. This feature induces the undercurrent to be farther west after detaching from the bottom at Cape St. Vincent, instead of turning northward. The undercurrent cannot extend farther west since it is blocked by topographic features at its southwest side, in particular by one of the Horseshoe Seamounts, the Gorringe Bank (See Fig. 1). At day 300, the meddy at the Estremadura Promontory detached from the undercurrent and a meddy began to form north of Cape St. Vincent. The results in experiment A1* strongly support the argument that topographic features play a key role in meddy formation processes.

The major difference observed in the modeled Mediterranean outflow between experiment A1* and experiments A1, A2, A3, and A4 appears to be the increased mixing with NACW in A1* within the Gulf of Cadiz, leading to a more buoyant undercurrent in the vicinity of Cape St. Vincent. The final buoyancy of the undercurrent after mixing with the NACW, and the stratification of the ambient North Atlantic, determine the depth at which the undercurrent will flow neutrally buoyant into the North Atlantic. The undercurrent in A1* is found to lie 200–400 m shallower and to be faster than in A1, A2, A3, and A4. The meddy activity observed in experiment A1* suggests that meddy formation is very sensitive to the depth and velocity of the neutrally buoyant Mediterranean undercurrent in the North Atlantic and its subsequent interaction with the local topographic features. To further investigate this issue, experiments A5 and A6 were performed in order to produce a more buoyant outflow by altering the entrainment parameterization in A5 and the prescribed Mediterannean outlfow in A6.

In experiment A5, the entrainment parameterization E5 (Section 3) is used to increase the turbulent entrainment velocities of ambient water into the outflow without the artifice of altering the mixing frequency. The increased strength of the mixing indeed produces a more buoyant outflow when compared to that seen in experiments A1, A2, A3, and A4 in the vicinity of Cape St. Vincent, lying between depths of 400 and 1200 m. The Mediterranean outflow properties at section 8.8°W after 200 days of simulation for A5 are summarized in Table 4.

The results of experiment A5 indicate that increased mixing does indeed lead to meddy activity in the region. Fig. 15 illustrates the horizontal velocity distribution in layer 16 ($\sigma_\Theta = 27.64 \text{ kg m}^{-2}$) at days 70, 150, 210, and 300 in experiment A5. The same topographic features again seem to

Table 4
Mediterranean outflow properties in experiments A1, A1*, A5 and A6 at section 8.8°W after 200 days of simulation

Exps/secns	S (psu)	σ_Θ (kg m^{-3})	Depth (m)	Max. vel (cm/s)	Trans. (Sv)
A1-8.8°W	36.1–36.5	27.38–27.82	500–1400	23	2.42
A5-8.8°W	36.1–36.6	27.32–27.74	400–1200	18	2.62
A1*-8.8°W	36.1–36.6	27.26–27.74	500–1200	22	3.2
A6-8.8°W	36–36.5	27.26–27.82	400–1200	20	2.23

Horizontal velocities for layer 16 (27.64 kgm^{-3})

(a): Day 70

(b): Day 150

(c): Day 210

(d): Day 300
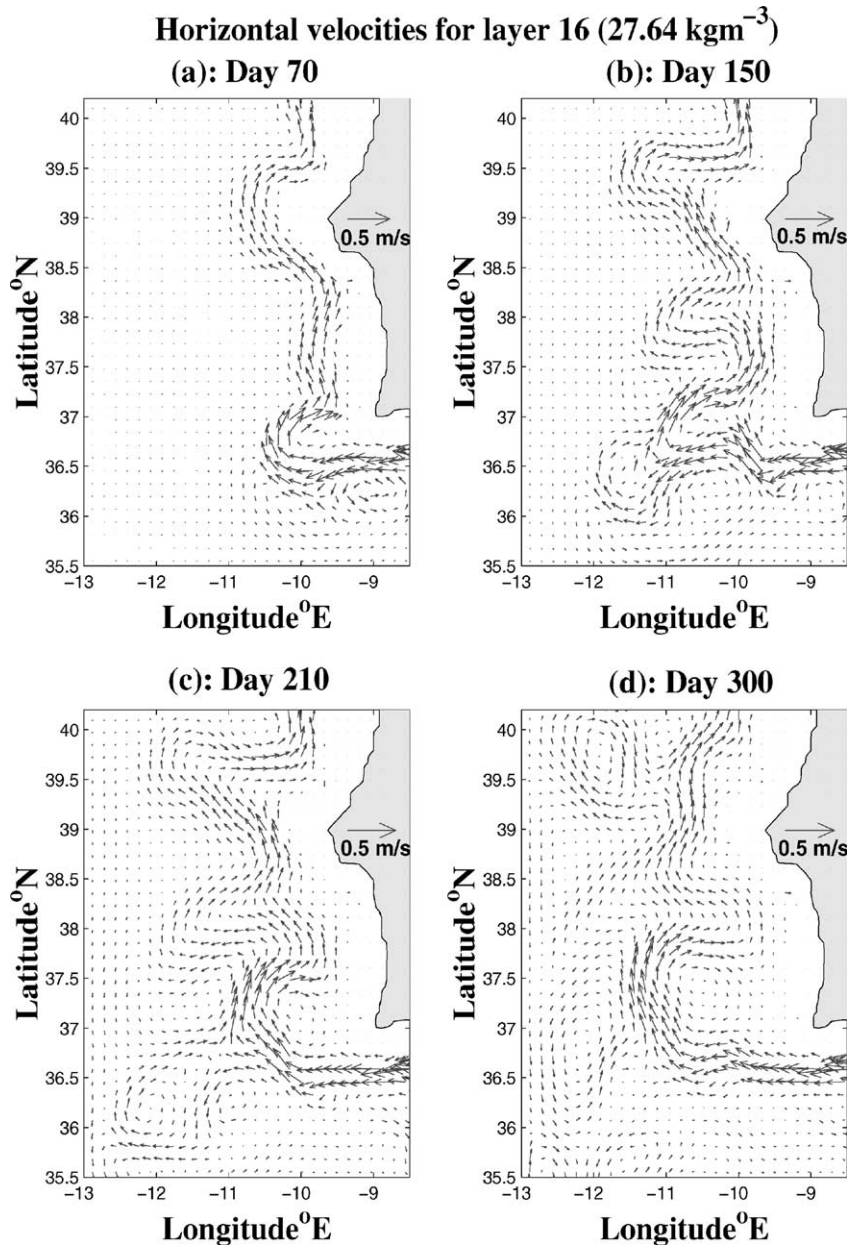

Fig. 15. Horizontal distribution of velocity in layer 16 ($\sigma_\Theta = 27.64$ kg m^{-3}) at days 70, 150, 210, and 300 in experiment A5. A new meddy formation site has emerged near the Gorringe Bank.

strongly influence meddy formation, with the Mediterranean undercurrent meandering west close to the Lisbon/Setubal Canyon and the Estremadura Promontory. An interesting new meddy formation site appears in the results, shown in Fig. 15b. The Mediterranean undercurrent bifurcates upon encountering the Gorringe Bank in its path. The northern (and stronger) part of the

current is driven northward by the meddy-like feature as it interacts with the Gorringe Bank, while the southern part flows around and interacts with the seamount forming a new meddy. At day 210, the meddy detaches from the undercurrent, which then assumes its regular course as illustrated in Fig. 14d. A meddy at the vicinity of Estremadura Promontory is also formed.

Experiment A6, like experiment A5, is also designed to obtain a more buoyant outflow downstream near Cape St. Vincent than that obtained in A1, A2, A3, and A4. However, instead of increasing the mixing by altering the entrainment mixing parameterization as in A5, experiment A6 is forced with a more buoyant and fresher outflow originating from the source at the western end of the Gibraltar Strait. The choice of a different outflow property at the western end of the strait can be justified by the variable mixing between the outflow and the overlying water that occurs in time within the strait (Send and Baschek, 2001). In A6, the potential density (σ_Θ) of the outflow is set to 28.40 kg m^{-3} and the salinity (S) to 37.8 psu (versus 28.94 kg m^{-3} and 38.4 psu in A1–A5). One therefore expects less mixing of the lighter gravity current within the Gulf of Cadiz than in experiments A1, A2, A3, and A4, but still a more buoyant undercurrent flowing in the North Atlantic. The Mediterranean undercurrent properties for A6 at day 200 at section 8.8°W are summarized in Table 4. Although the outflow in A6 is forced with a lower value of salinity (37.8 psu), the salinity of the undercurrent in A6 is found to be not significantly different at 8.8°W from that of the other experiments. This can be attributed to the expected reduction of mixing of the outflow with the NACW in A6, which is also witnessed from the low transport outflow value estimated at 8.8°W. Meddy formation is evident again in experiment A6 with a similar pattern to that of A5. The undercurrent in Fig. 16, however, appears to be much weaker within the North Atlantic (velocities reduced by up to 50%) compared to that of A1* and A5. The reduced speed of the undercurrent leads to smaller rotation speeds of the meddies. In Fig. 16, the undercurrent bifurcates at the Gorringe Bank and sheds a meddy at the southern site of the seamount, while another meddy forms to the north at the Estremadura Promontory.

4.5. Fluctuating outflow at the Strait of Gibraltar

Meddies detach from the Mediterranean undercurrent in experiments A1*, A5, and A6, at formation sites that appear to be regions where the undercurrent feels the influence of topography. Stern and Chassignet (2000) show that the downstream convergence of velocities of a boundary current, caused by topographic effects or by fluctuations of the current at the source, is a possible mechanism that could account for the separation of eddies from the current. Topographic effects clearly influence meddy formation in the experiments performed thus far, but a fluctuating source producing downstream convergence in the current velocities is also not an unrealistic scenario for the Mediterranean outflow. The semi-diurnal M2 tide considerably influences the flow at the Strait of Gibraltar (Bryden et al., 1994), sometimes completely reversing the direction of the outflow. Experiment A7 is identical to experiment A1*, but with the initial outflow zonal velocity at the source at 6°W varying sinusoidally between 0 and 120 cm s^{-1} with a period of 0.5 days. The interface between the Mediterranean outflow and the overlying water at the source is kept constant and geostrophically adjusted to the mean outflow zonal velocity of 60 cm s^{-1} at the strait. This choice was made considering that the inertial period at the Strait of Gibraltar is approximately 0.9 days and limited geostrophic adjustment occurs with a tidal period of 0.5 days. The inflow velocities of the top layers into the Mediterranean at the source also vary
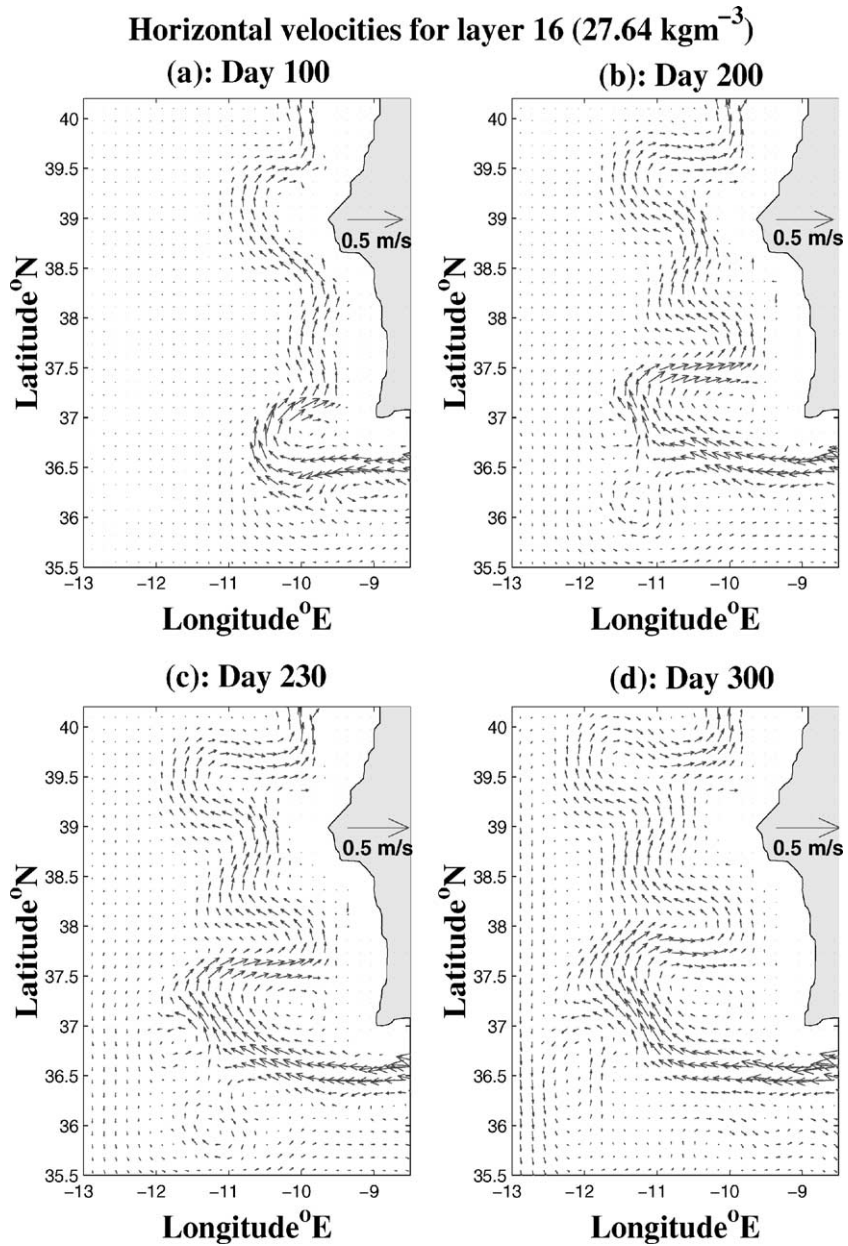
Fig. 16. Horizontal distribution of velocity in layer 16 ($\sigma_\Theta = 27.64$ kg m^{-3}) at days 100, 200, 230, and 300 in experiment A6.

sinusoidally, with a phase difference of 180° (for numerical convenience rather than realism in depicting the barotropic tidal flows).

Experiment A7 produces much greater meddy activity within the region than does experiment A1*. Fig. 17 illustrates horizontal velocities for layer 15 after 60, 120, 220, and 300 days of
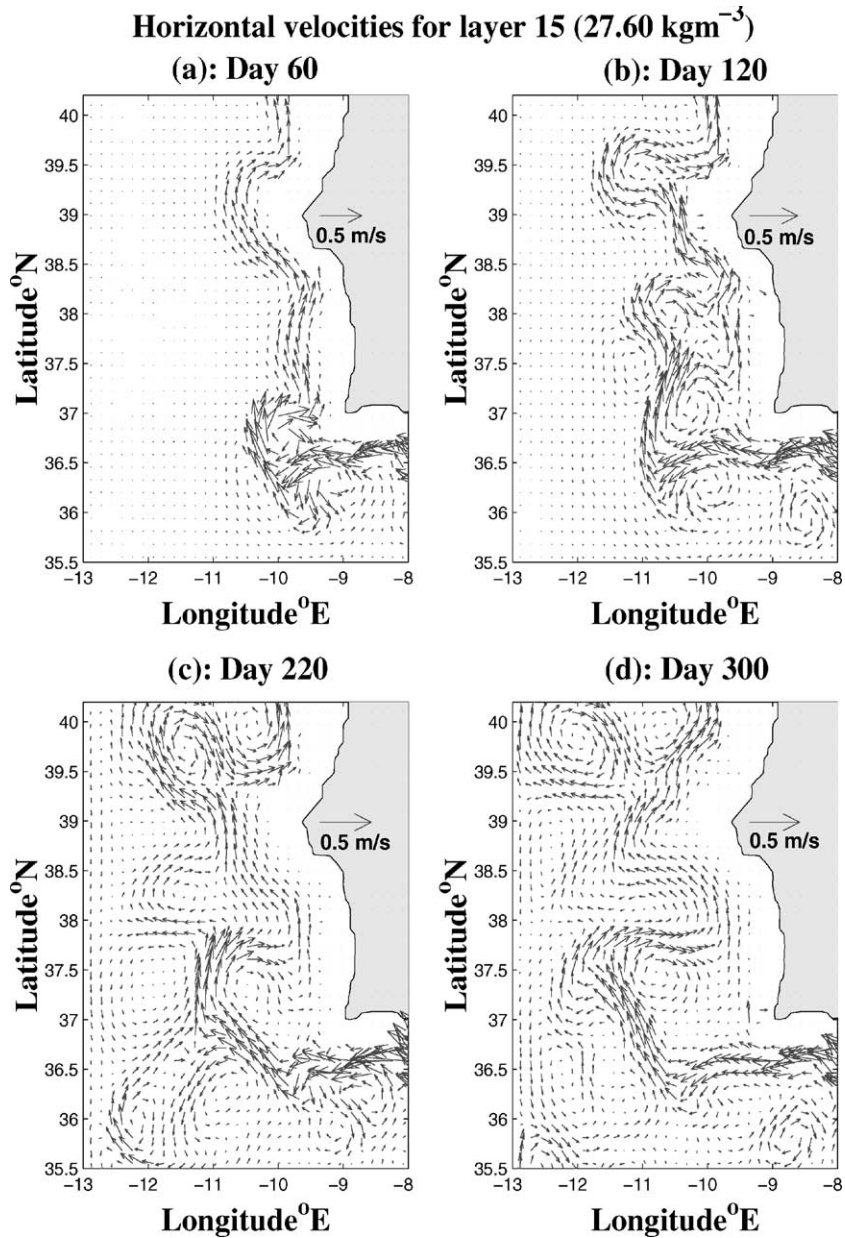
Fig. 17. Horizontal distribution of velocity in layer 15 ($\sigma_\Theta = 27.60 \text{ kg m}^{-3}$) at days 60, 120, 220, and 300 in experiment A7. The fluctuating outflow at the source clearly enhances meddy activity.

simulation. After 60 days, a dipole (anticyclonic meddy + cyclone) forms at the tip of Cape St. Vincent, where the Mediterranean outflow detaches from the bottom terrain to flow neutrally buoyant into the North Atlantic. This particular meddy propagates eastward, as shown in Fig. 17b. Fig. 17c illustrates another meddy forming in the same fashion and again propagating

eastward (Fig. 17d). A meddy is formed and detaches from the undercurrent in the vicinity of the Lisbon/Setubal Canyon at 38.25°N in experiment A7 (Fig. 17c), in contrast to A1*, A5, and A6, in which separation at this location was never achieved. Two more meddies are formed in the same regions as seen in previous experiments: one at the Estremadura Promontory and the other at the Gorringe Bank as a result of the bifurcation of the Mediterranean undercurrent. The increased meddy activity in the region indicates that the results of experiment A7 agree with the work of Stern and Chassignet (2000), i.e., flow convergences within the plume caused by a variable outflow from the Strait lead to enhanced meddy formation.

The frequency of the mixing was found to play a significant role in the formation of meddies (Section 4.4), since experiment A1 with a frequency equal to 1 did not produce any meddies, while an identical experiment, A1*, with frequency 1/144 did generate several. The question then arises as to whether a fluctuating source with a frequency equal to 1 can generate meddies. Experiment A8 is identical to experiment A1 except for the Mediterranean outflow, which is forced as a fluctuating source at the Strait of Gibraltar as in A7. No meddies are formed in A8. The Mediterranean undercurrent in A8, as in A1, lies deeper in comparison to its depth in the meddy-producing experiments A1*, A5, A6, and A7. This indicates once more how important the depth and velocity structure of the Mediterranean undercurrent, and therefore its interaction with the local topographic features, is in the production of meddies.

5. Summary and discussion

In this paper, the results of realistic experiments performed with MICOM in the vicinity of the Gulf of Cadiz, intending to simulate the Mediterranean outflow, have been discussed. The modeled Mediterranean outflow, forced as a source at the west end of the Strait of Gibraltar, flows down the continental slope and into the Gulf of Cadiz while mixing with the overlying North Atlantic Central Water. The outflow characteristics, such as buoyancy, salinity, transport, and depth were compared at different sections along its path to observations from Baringer and Price (1997) and were found to be in good agreement. This suggests that the Hallberg (2000) scheme using the Turner (1986) entrainment parameterization is able to reproduce basic characteristics of the mixing between bottom gravity currents and the environment. Several sensitivity experiments that the Mediterranean undercurrent's properties at Cape St. Vincent, after mixing with the NACW, appear to be rather sensitive to the entrainment parameterization (particularly to the critical Richardson number and to a lesser extent to the entrainment rates). To investigate whether this sensitivity is realistic or not, or even to comment on the original Turner (1986) entrainment parameterization effectiveness, would require combined efforts involving numerical simulations and observations (see Özgökmen and Chassignet (2002) for details).

It is, however, interesting to speculate on how the Turner (1986) entrainment parameterization (TP hereafter) compares to the K-profile parameterization (KPP hereafter) of Large et al. (1994) which is widely used in ocean models. KPP is derived from a wide range of oceanic observations, whereas TP is based primarily on small-scale laboratory measurements of entraining gravity currents. There are a number of decidedly non-oceanic aspects to the TP measurements, notably a lack of rotation, the large aspect ratio, a possible exaggeration of viscous effects, and a lack of interaction with small- or large-scale topographic irregularities or background (e.g., tidal) flows.

These differences might imply that KPP is more pertinent to all oceanic situations, or they might imply that TP is more pertinent to entraining gravity currents such as the Mediterranean outflow. However, the interior mixing parameterization of KPP is not a fit to oceanic observations, but rather a broad representation of them, since it was explicitly developed for coarse resolution ocean models. KPP, for example, assumes that regions with the smallest Richardson numbers cannot be resolved. Specifically, the Richardson number dependence in KPP is much less step-like than observed, and therefore the smallest Richardson numbers in KPP will induce less mixing, while enhanced mixing extends to much larger Richardson numbers. This is appropriate for *z*-coordinate models in which one can assume that the resolved Richardson numbers will be much larger than the highest small-scale observed values, and that large-scale regions with very small Richardson numbers are very uncommon (see p. 373 of Large et al. (1994) for details). These assumptions are not, however, necessarily appropriate to a dense overflow in an isopycnic coordinate model. The real skill of an isopycnic coordinate ocean model in representing a dense overflow lies in the migration of its vertical resolution into regions of high shear, within which the model can resolve regions of very small Richardson number. It is therefore logical to use this capability to parameterize the mixing rates as accurately as possible. From this standpoint, the TP parameterization is much more appropriate than KPP for representing dense overflows in isopycnic coordinate models.

The present investigation can be extended in several directions. First, more process studies can be carried out in the region for further study of the Mediterranean outflow characteristics, such as transport, buoyancy, salinity, temperature, and separation into different cores, within the Gulf of Cadiz and into the North Atlantic. Second, the striking similarity to observations of the results obtained for the Mediterranean outflow strongly encourage numerical simulations of other marginal sea overflows. The Northern Atlantic marginal sea overflows at the Denmark Strait and Faroe Bank Channel make up the deep core of the Deep Western Boundary Current, the transport estimates and properties of which are of considerable importance to the global oceanic circulation. Meddy formation is not yet fully understood, and a 3-dimensional primitive equation model can be a powerful tool in shedding light on the dynamics of such a process. Meddy propagation and maintenance of the Mediterranean salt tongue are also an important issue that can be addressed in further studies. The observed westward meddy translation is also believed to be responsible for the westward salt flux that maintains the Mediterranean salt tongue in the North Atlantic (Richardson et al., 2000). For the purpose of studying such processes, a full North Atlantic basin numerical model is necessary.

Meddies do form in several of the experiments as part of the modeled Mediterranean undercurrent detach from the main core to form anticyclonic subsurface vortices. In all such experiments, meddy formation appears to be highly influenced by certain topographic features in the region, such as the Lisbon/Setubal Canyon and the Estremadura Promontory along the Portuguese coast. Meddies were also observed forming near Cape St. Vincent, where the Mediterranean outflow detaches from the bottom. Another result noted both in experiments and reality is the bifurcation of the Mediterranean undercurrent upon encountering the Gorringe Bank in its path. The southern part of the undercurrent flows around the seamount after the bifurcation and forms meddies.

The experiments performed in this study indicate that meddy formation in the region is very sensitive to the depth at which the Mediterranean undercurrent lies in the North Atlantic. This

depth depends upon the ambient stratification of the region, the characteristics of the initial Mediterranean outflow at the Strait, and the amount of mixing between the outflow and NACW. A Mediterranean undercurrent lying at shallower depths produces a much higher meddy activity in the region, upon interacting with the local topographic features. Finally, it was found that, in agreement with the results of Stern and Chassignet (2000), there is an increase in meddy activity following the inclusion of fluctuations of the Mediterranean undercurrent at the Strait of Gibraltar.

Until recently, most simulations of the North Atlantic ocean (including those using MICOM), have represented the Mediterranean outflow by a buffer zone inside the Gulf of Cadiz. Paiva et al. (2000) show that a buffer zone can be problematic in maintaining the Mediterranean salinity tongue in the North Atlantic and suggest that the best solution would be the inclusion of the Mediterranean Sea itself in the model domain. Jia (2000) also show that the water mass transformations associated with the restoring toward observations within the Gulf of Cadiz induced an Azores-like current. This led Özgökmen et al. (2001) to argue that the primary cause for the Azores current could be the water mass transformation associated with the entrainment of lighter water by the Mediterranean outflow in the Gulf of Cadiz. However, the inclusion of the Mediterranean Sea in a large-scale ocean model requires the explicit parameterization of the mixing of the Mediterranean outflow with the NACW, a requirement that the Hallberg (2000) scheme with the TP parameterization satisfies for isopycnic coordinate ocean models, as demonstrated in this study. The Hallberg (2000) scheme has been implemented with success in the MICOM North and Equatorial high resolution (1/12°) model and results similar to these and therefore to observations have been obtained regarding the Mediterranean outflow and meddy formation in the region.

Acknowledgements

References

Ambar, I., Howe, M.R., 1979. Observations of the Mediterranean outflow—1: mixing in the Mediterranean outflow. Deep-Sea Res. 26A, 535–554.

Baringer, M.O., Price, J.F., 1997. Mixing and spreading of the Mediterranean outflow. J. Phys. Oceanogr. 27, 1654–1677.

Baschek, R., Send, U., Lafuente, J.G., Candela, J., 2001. Transport estimates in the Strait of Gibraltar with a tidal inverse model. J. Geophys. Res. 106, 31033–31044.

Bleck, R., Rooth, C., Hu, D., Smith, L.T., 1992. Salinity-driven thermocline transients in a wind- and thermohaline-forced isopycnic coordinate model of the North Atlantic. J. Phys. Oceanogr. 22, 1486–1505.

Bleck, R., Chassignet, E.P., 1994. Simulating the oceanic circulation with isopycnic coordinate models. In: The Oceans: Physical and Chemical Dynamics and Human impact. The Pennsylvania Academy of Science, pp. 17–39.

Bower, A.B., Armi, L., Ambar, J., 1997. Lagrangian observations of meddy formation during a Mediterranean undercurrent seeding experiment. J. Phys. Oceanogr. 27, 2545–2575.

Bryden, H.L., Candela, J.C., Kinder, T.H., 1994. Exchange through the Strait of Gibraltar. In: Progress in Oceanography, vol. 33. Pergamon Press, Oxford, pp. 201–248.

Chassignet, E.P., Garraffo, Z., 2001. Viscosity parameterization and the Gulf Stream separation. In: Muller, P., Henderson, D. (Eds.), ''From Stirring to Mixing in a Stratified Ocean''. Proceedings 'Aha Huliko'a Hawaiian Winter Workshop. Universiy of Hawaii, January 15–19, 2001, pp. 37–41.

D'Asaro, E.A., 1988. Generation of submesoscale vortices: a new mechanism. J. Geophys. Res. 93, 6685–6693.

Gawarkiewicz, G., Chapman, D.C., 1995. A numerical study dense water formation and transport on a shallow, sloping continental shelf. J. Geophys. Res. 100, 4489–4507.

Hallberg, R., 2000. Time integration of diapycnal diffusion Richardson number dependent mixing in isopycnal coordinate ocean models. Mon. Weath. Rev. 128, 1402–1419.

Jia, Y., 2000. Formation of an Azores current due to Mediterranean overflow in a modeling study of the North Atlantic. J. Phys. Oceanogr. 30, 2342–2358.

Jiang, L., Garwood Jr., R.W., 1995. A numerical study of three-dimensional dense bottom plumes on a Southern Ocean continental slope. J. Geophys. Res. 100, 18471–18488.

Jiang, L., Garwood Jr., R.W., 1996. Three-dimensional simulations of overflows on continental slopes. J. Phys. Oceanogr. 26, 1214–1233.

Jungclaus, J.H., 1999. A three-dimensional simulation of the formation of anticyclonic lenses (Meddies) by the instability of an intermediate depth boundary current. J. Phys. Oceanogr. 29, 1579–1598.

Jungclaus, J.H., Backhaus, J.O., 1994. Application of a transient reduced gravity plume to the Denmark Strait overflow. J. Geophys. Res. 99, 12375–12396.

Jungclaus, J.H., Mellor, G., 2000. A three-dimensional model study of the Mediterranean outflow. J. Mar. Sys. 24, 41–66.

Killworth, P.D., 1977. Mixing on the Weddell Sea continental slope. Deep-Sea Res. 24, 427–448.

Kinder, T.H., Parilla, G., 1987. Yes, some of the Mediterranean Outflow does come from great depth. J. Geophys. Res. 92, 2901–2906.

Large, W.G., McWilliams, J.C., Doney, S.C., 1994. Oceanic vertical mixing: a review and a model with a nonlocal boundary layer parameterization. Rev. Geophys. 32, 363–403.

Levitus, S., 1982. Climatological atlas of the world ocean. NOAA Prof. Paper No 13, US Government Printing Office, 173 pp.

Madelain, F., 1970. Influence de la topographie du fond sur l'ecoulment Mediterraneen entre le Detroit de Gibraltar et le Cap Saint-Vincent (Influence of topography on the Mediterranean outflow between the Strait of Gibraltar and Cape St. Vincent). Cah. Oceanogr. 22, 43–61.

Özgökmen, T.M., Chassignet, E.P., Rooth, C.G.H., 2001. On the connection between the Mediterranean outflow and the Azores current. J. Phys. Oceanogr. 31, 461–480.

Özgökmen, T.M., Chassignet, E.P., 2002. A numerical study of two-dimensional turbulent bottom gravity currents. J. Phys. Oceanogr. 32, 1460–1478.

Paiva, A.M., Chassignet, E.P., Mariano, A.J., 2000. Numerical simulations of the North Atlantic subtropical gyre: sensitivity to boundary conditions. Dyn. Atmos. Oceans 32, 209–237.

Price, J.F., Baringer, M.O., 1994. Outflows and deep water production by marginal seas. Prog. Oceanogr. 33, 161–200.

Richardson, P.L., Bower, A.S., Zenk, W., 2000. A census of Meddies tracked by floats. Prog. Oceanogr. 45, 209–250.

Seidler, G., 1968. Haufigkeitsverteil von Wasserarten im Ausstrombereich von Meeresstrassen. Kiel. Meeresforch. 24 (2), 59–65.

Send, U., Baschek, B., 2001. Intensive shipboard observations of the flow through the Strait of Gibraltar. J. Geophys. Res. 106, 31017–31032.

Stern, M.E., Chassignet, E.P., 2000. Mechanism of eddy separation from coastal currents. J. Mar. Res. 58, 269–295.

Smith, P.C., 1975. A streamtube model for bottom boundary currents in the ocean. Deep-Sea Res. 22, 853–873.

Turner, J.S., 1986. Turbulent entrainment: the development of the entrainment assumption, and its application to geophysical flows. J. Fluid Mech. 173, 431–471.

Willebrand, J., Barnier, B., Böning, C., Dietrich, C., Herrmann, P., Killworth, P.D., LeProvost, C., Jia, Y., Molines, J.-M., New, A.L., 2001. Circulation characteristics in three eddy-permitting models of the North Atlantic. Prog. Oceanogr. 48, 123–161.
Yu, Z., Schopf, P., 1997. Vertical eddy mixing in the tropical upper ocean: its influence on zonal currents. J. Phys. Oceanogr. 27, 1447–1458.